NCAT Report 17-04

HIGH-MODULUS ASPHALT CONCRETE (HMAC) MIXTURES FOR USE AS BASE COURSE

By
Fabricio Leiva-Villacorta
Adam Taylor
Richard Willis

June 2017

National Center for Asphalt Technology
NCAT
at AUBURN UNIVERSITY

277 Technology Parkway ▪ Auburn, AL 36830

HIGH-MODULUS ASPHALT CONCRETE (HMAC) MIXTURES FOR USE AS BASE COURSE

NCAT Report 17-04

By:

Fabricio Leiva-Villacorta, PhD
Assistant Research Professor
National Center for Asphalt Technology at Auburn University

Adam Taylor, P.E.
Assistant Research Engineer
National Center for Asphalt Technology at Auburn University

Richard Willis, PhD
Director of Pavement Engineering & Innovation
National Asphalt Pavement Association

June 2017

ACKNOWLEDGEMENTS

DISCLAIMER

TABLE OF CONTENTS

ABSTRACT

Recent studies on long-life flexible pavements indicate that it may be advantageous to design and construct asphalt mixtures comprising the underlying layers in such a manner that very high modulus mixtures are produced. The French have been experimenting with and designing pavements with high-modulus bases since the 1980s. This study considered the engineering properties of asphalt mixtures produced using a European specification for high-modulus asphalt concrete (HMAC) mixtures and used as base course. This specification includes volumetric requirements such as asphalt content and air voids, but there are also requirements for engineering parameters that address performance requirements such as rutting and fatigue cracking. The purpose of this study was to investigate the design of asphalt mixtures having higher modulus. The study was limited to a laboratory performance evaluation and a theoretical modeling component where the results were used to indicate potential field performance.

A comprehensive literature study was performed to assess the current state-of-the-practice on HMAC mixture design, pavement design, laboratory performance tests, and full scale pavement performance. The experimental plan included a variety of mixtures with different material and binders such that higher moduli were obtained compare to conventional mixtures. The plan included a French mixture with a stiff binder (PG 88-16), two mixtures containing 35% RAP both with polymer-modified binders but one high polymer content (HiMA), another mixture containing 25% RAP and 5% RAS with a polymer-modified binder, and finally, a 50% RAP mixture with a polymer-modified binder. The laboratory testing program evaluated binder performance grade, mixture stiffness over a wide temperature range, fatigue cracking, and permanent deformation. In addition, AASHTOWare Pavement ME Design software was used to determine how a high-modulus base would affect predicted performance of asphalt pavements.

The results of this study indicated that European mix design standard methods and specifications were successfully implemented on local (U.S.) virgin and recycled materials. In addition, increased stiffness of high modulus mixtures improves mechanistic-empirical predicted performance of pavement in rutting, fatigue cracking, and ride quality. However, it was determined that performance of new materials cannot be reliably modelled with the current transfer functions and further field validation is required.

1. INTRODUCTION

Currently in the United States, asphalt paving mixtures are primarily designed using the Superpave system where the proportioning of components relies mainly on volumetric properties. Early Superpave implementation focused primarily on rutting resistance. Mixture designs for moderate and high traffic pavements were designed for improved rutting resistance by specifying a higher grade of asphalt binder and higher quality aggregates. Most highway agencies now report that rutting problems have been virtually eliminated. However, there have been growing concerns that the primary mode of distress for asphalt pavements is cracking of some form or another. There are several possible contributing factors to increased cracking, including issues with mixture designs, increased use of recycled materials, problems with the quality of construction, and failure to adequately address underlying pavement distresses during pavement rehabilitation. It is now well recognized that current mixture design practices have some shortcomings.

Most state departments of transportation (DOTs) currently utilize volumetric criteria for asphalt mixture designs that follow the Superpave mixture design methods of AASHTO M 323 and R 35 with some modifications. In response to pavement durability issues, many DOTs have modified their design and acceptance requirements to obtain more durable and high crack-resistant mixtures by increasing the asphalt content of the lower layer of hot-mix asphalt, commonly referred to as rich-bottom mixtures. Rich-bottom mixtures are made with the same grade of asphalt binder but are designed at a lower air void content so as to increase the design asphalt content by 0.6% to 0.8%.

This study considered the engineering properties of asphalt mixtures produced using a European specification for high-modulus asphalt mixtures and used as base course. This specification includes volumetric requirements such as asphalt content and air voids, but there are also requirements for engineering parameters that address performance requirements such as rutting and fatigue cracking. High-modulus asphalt is routinely produced with hard asphalt binders, PG 88 or higher, for critical high temperature properties. In this study, an effective hard asphalt binder was obtained by combining polymer-modified asphalt with several contents of RAP (between 25% and 50%) and utilized in a high-modulus mixture produced following French standard procedures.

In the 1980s, the French Public Works Research Institute or Laboratoire Central des Ponts et Chaussées (LCPC) developed high-modulus mixtures, referred to as *Enrobé à Module Élevé (EME).* The objective for this type of new mixture was improved mechanical properties to include high-modulus, good fatigue behavior, and excellent resistance to rutting. High stiffness and improved fatigue resistance allow a decrease in pavement thickness for both new construction and for rehabilitation. One goal of the EME developers was to reduce geometric constraints (overhead clearance constraints) during rehabilitation. Early trials of EME occurred in the mid-1970s and by the early 1980s had developed into a new mixture type. A specification was set by the early 1990s and in the late 1990s the mixture had become part of the standard catalog of mixtures used in

pavement structural design for high traffic pavements, 20 million equivalent single axle loads (ESALs) or greater.

In the United States, agencies are beginning to adopt the Mechanistic Empirical Pavement Design Guide (MEPDG) for determining pavement structural thickness. Unlike the previous structural design method, typically AASHTO 1993, which only considered mixture properties indirectly, the MEPDG makes direct use of mixture properties as part of the structural pavement design. This study compares an MEPDG pavement structural design using only Superpave mixtures and several high-modulus mixtures for the base course.

2.   OBJECTIVE

The objective of this project was to evaluate the current mixture design methodology of high-modulus base layers and evaluate potential effects on performance. In order to successfully analyze the effect of high-modulus mixtures as base courses, the following tasks were completed on this project:

1. Literature review: A literature study was performed to assess the current state-of-the-practice. This included information from published journals, technical reports, articles, presentations, as well as personal communications and interviews with contractors and agencies that have successfully implemented high-modulus mixtures in their pavement structures.
2. Provide recommendations of mixture design and structural design procedures: Data and resources gathered during the literature review were used to develop material selection and mixture design procedures for a high-modulus mixture that would be resistant to the tensile strains at the bottom of the asphalt pavement structure.
3. Laboratory study: Engineering properties of high-modulus mixtures were determined and design procedures were assessed using laboratory performance tests.
4. Pavement design and analysis: AASHTOWare Pavement ME Design software was used to determine how a high-modulus base would affect predicted performance of asphalt pavements.

3.   STATE-OF-THE-PRACTICE

High-modulus asphalt concrete (HMAC) was originally developed in the 1980s at a time when France was looking to design high performance asphalt mixtures to increase the life span of conventional asphalt pavements or reduce the necessary thickness required to carry the increasing loads seen on European highways. Although these mixtures were designed to serve as either asphalt base or binder courses, they were eventually also used in wearing courses in the mid-1980s, but these are outside of the scope of this report (EAPA, 2005; Nkgapele et al., 2012; Corte, 2001).

In the 1990s, the French developed a standard for EME mixtures (Denneman, 2011; Petho and Denneman, 2013). This standard had two classes of EME mixtures. Class 1 was a low fatigue resistance mixture while Class 2 was a higher fatigue resistant mixture. The main difference

between these two classes was the binder content of the mixtures. In 2007, a European Standard (EN 13108-20) was developed (Brosseaud, 2012; Guyot 2013).

To date, numerous European countries such as France, Austria, the Czech Republic, Denmark, Ireland, Italy, Netherlands, Portugal, and the United Kingdom have all had positive experiences using this material; however, each country has a slightly different approach to mixture design and performance criteria, as expected. Generally, these mixtures have been successfully incorporated at times when low quality aggregates are available to reinforce the mixtures, industrial areas are subjected to heavy loads, and when existing pavements need to be reinforced during rehabilitation or reconstruction (Brosseaud, 2012; EAPA, 2005; Petho and Denneman, 2013). Case studies at airports have also been conducted to improve runway and taxiway durability (EAPA, 2003; Guyot, 2013).

3.1   Mixture Design

As with most asphalt mixtures, asphalt and aggregate are the two primary constituents used in HMAC. However, unlike Marshall mixture design or Superpave mixture design, the mix design is not driven by volumetric properties as much as it is driven by trying to pass performance-based specifications. This method of mixture design is actually developed to assess performance in relation to the loading and environmental conditions the mixture may experience. This type of design methodology reduces barriers to innovation, promotes mixture performance, and encourages the efficient use of resources (Denneman et al., 2011). Figure 1 provides a flowchart of the basic process of developing an HMAC mixture. This section of the literature review will explain each portion of the flowchart. Since the French have the most experience with developing HMAC mixtures, this literature review will follow the French method and show how South Africa has taken the European standard and adopted it to follow ASTM and AASHTO methods.
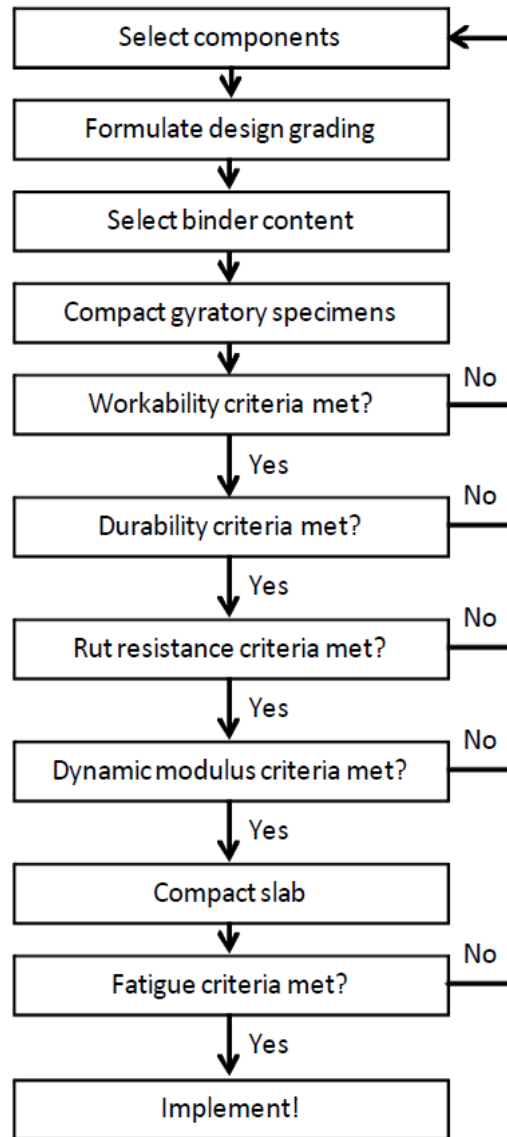
Figure 1 HMAC Mixture Design Process (Denneman et al., 2012)

3.1.1 Aggregate Selection

In many European countries, South Africa, and in Australia, HMAC incorporates fully crushed aggregate due to the importance of both surface area and texture. These two properties aid in increasing the voids in the mineral aggregate (VMA), which must be sufficient to accommodate the higher asphalt binder content in the mixtures. Aggregate selection guidelines have been developed to aid in properly choosing the skeletal structure. Table 1 shows an example of HMAC aggregate selection criteria in South Africa.

Table 1 HMAC Aggregate Selection Criteria (Denneman et al., 2011)

Property	Test	Method	Criteria
Hardness	Fines aggregate crushing test: 10% FACT	TMH1, B1	≥ 160 kN
	Aggregate crushing value ACV	TMH1, B1	≤ 25%
Particle shape & texture	Flakiness index test	SANS 3001	≤ 25%
	Particle index test	ASTM D3398	>15 10-15 (Delorme, 2007)
Water absorption	Water absorption coarse aggregate (>4.75 mm)	TMH1, B14	≤ 1.0%
	Water absorption fine aggregate	TMH1, B14	≤ 1.5%
Cleanliness	Sand equivalency test	TMH1, B19	≥ 50

While these criteria were developed to ensure high quality aggregates are used in HMAC, countries such as Latvia were not permitted to use dolomite aggregate in high modulus mixtures. A small-scale research project was conducted using locally available aggregate in Latvia to see if either using a polymer or hard binder in conjunction with dolomitic aggregate might equal or better the performance of a reference mixture that represents a typical mixture (Haritonovs et al., 2014).

Mixtures were designed using the Marshall mixture design method and subjected to TSR, rutting, and fatigue performance testing. The reference mixture was not designed using the HMAC methodology; thus, it had a lower asphalt content. When compared to the HMAC mixtures, the reference mixture performed better with respect to rutting, but the lower binder content caused reduced fatigue capacity. The HMAC with a polymer-modified binder performed better than the hard binder in rutting. Overall, the study results showed that using a local aggregate that might not be considered high quality might be acceptable in an HMAC mixture if specification requirements are still met (Table 2) (Haritonovs et al., 2014).

Table 2 Compliance with Sustainable Pavement for European New Member States (SPENS) Requirements (Haritonovs et al., 2014)

Parameter	Mixtures				Requirement
	PMB 10/45-65		B20/30		
	HMAC-1/1	HMAC-1/2	HMAC-2/2	HMAC-2/3	
Void content, %	3.9	3.7	3.9	3.7	3.0 – 5.0
Rut resistance, mm/1000 cycles	0.04	0.04	0.14	0.22	0.03-0.25
Stiffness (10°C, 10 Hz) MPa	16700	16100	17100	17900	Min 14000
Fatigue (10°C, 10Hz), μmm/mm	130	130	130	130	Min. 130 at 1 million Cycles
Water Sensitivity, TSR, %	100	100	98	94	TSR 80

During an HMAC implementation study that consisted of testing HMAC with off-scale limestone, granite, crushed cobblestone, steel slag, and basalt, it was determined that lower quality aggregates could be used because HMAC mixture design moves away from empirical mixture

design and progresses to competent mixture design. This provides the opportunity to pair weaker or lower quality materials with higher quality materials to ensure pavement performance (Bankowski et al., 2009).

A common concern with HMAC relates to the inclusion of reclaimed asphalt pavement (RAP). Early experiments containing 30% RAP showed issues with compaction, resistance to water, and fatigue damage (Des Croix, 2004). Since that time, other limited laboratory studies have shown that RAP can be included up to 40%, and 25% RAP has been included in field studies with success. However, much of this research caveats the conclusions by stating that not all binders and RAP sources are equivalent, and this must be evaluated on a mixture by mixture basis to ensure performance of the mixture, which is the primary goal (de Visscher et al., 2008; Bueche et al., 2008). Additionally, past work has shown that improper characterization of RAP might influence low field binder contents compared to target contents during production (Nkgapele et al., 2012).

One study recently tested mixtures that had been placed in the field using 0%, 50%, and 65% RAP. When the mixture was tested in the laboratory, all of the performance requirements for HMAC mixtures were met even at higher RAP contents. While this work was preliminary, it did suggest that RAP could be used to produce an EME mixture; however, like any high recycle mixture, it is important to have good homogeneity, control, and material characterization (Brosseaud et al., 2012).

Another study compared HMAC mixtures with 0, 15, 30, and 50% RAP. These mixtures were analyzed mechanically for toughness (Fenix test), stiffness, rutting, moisture damage, and fatigue resistance. The study concluded that increasing RAP content using a softer binder did not have a negative impact on mechanical mixture performance; however, the research stated that plant logistics may make reaching 50% RAP unattainable. When the mixtures were attempted at a local batch plant, the 50% RAP mixture could not be produced because the non-heated RAP would not thoroughly mixture with the heated aggregate and bitumen for material transfer of the aged binder on the RAP (low RAP binder activation); thus, plant considerations may limit RAP use in HMAC similar to standard asphalt mixtures (Miro et al., 2011).

3.1.2   Designing a Gradation

When considering the gradation requirements used in numerous countries, deviations occur. For example, the grading envelopes in France (Delorme et al., 2007) are different than those of the United Kingdom (Sanders and Nunn, 2005). Other challenges in directly translating specifications from the French versions are differences in nomenclature and European sieve sizing.

South Africa developed a table for targeted grading curves that included both European and metric sieve sizes (Table 3). This allowed development of gradations like those in Europe; however, they could use their own equipment. Additionally, one should note that the French designs were based on the maximum sieve size with requiring 100% passing at 2D, 98-100% passing at 1.4D, and 85-98% pass at D (D = max sieve size).

Table 3 Target Grading Curves and Envelopes for HMAC Base Courses (Denneman et al., 2011)

Percent Passing Sieve Size	D = 10 mm			D = 14 mm			D = 20 mm		
	Min	Target	Max	Min	Target	Max	Min	Target	Max
6.7 mm	47	56	68	52	54	72	46	54	66
6.3 mm	45	55	65	50	53	70	45	53	65
4.75 mm	-	53	-	43	49	63	42	49	62
4.0 mm	-	52	-	40	47	60	40	47	60
2.36 mm	32	36	44	28	26	42	28	36	42
2.0 mm	28	33	38	25	33	38	25	33	38
0.075 mm	6.4	6.9	7.4	5.5	6.9	7.9	5.5	6.7	7.9
0.063 mm	6.3	6.7	7.2	5.4	6.7	7.7	5.4	5.7	7.7

D = max sieve size

3.1.3 Binder Selection and Richness Factor

European Standard EN 13924 governs binder selection for HMAC mixtures. Typically, 10/25 or 15/25 pen binders have been used in Europe (Denneman et al., 2011). In the 1980s, France began designing and producing the hard binder needed for these mixtures. In 1990, France produced 39,000 tons of the binder. By 2000, that value had grown to over 100,000 tons. The binder was originally developed through an air blowing process; however, this increased the brittleness of the binders and made them more susceptible to fatigue cracking. Since that time, vacuum distillation and propane-precipitated asphalt has been used to produce the stiff asphalt needed (Corte, 2003). Most of these binders had penetrations between 10 and 30 and softening points greater than 60 or 70°C (EAPA, 2005). Examples of typical hard asphalt characteristics before aging are given in Table 4. Rheological properties of common asphalts used in HMAC are provided in Table 5.

Table 4 Typical Hard Asphalt Characteristics (Before Aging) (Corte, 2001)

Penetration Grade	15/25	10/20	5/10
R&B Softening point (°C)	66	62 to 72	87
Pfeiffer IP (Penetration Index)	+0.2	+0.5	+1.0
Dynamic Viscosity at 170°C (mm^2/sec)	420	700	980
Complex Modulus at 7.8 Hz, IE*I, (MPa)			
0°C	425	700	980
10°C	180	300	570
20°C	70	110	300
60°C	0.4	0.7	7

Table 5 Rheological Characteristics of Seven 10/20 Asphalts and a 35/50 Asphalt (Corte, 2001)

	35/50	A	B	C	D	E	F	G
$|G^*|$ (15°C; 10 Hz) (MPa)	34.5	53.7	88	88	83.7	71.1	43.7	47.3
$|G^*|$ / sinδ (60°C; 5 Hz) (MPa)	0.016	0.131	0.184	0.247	0.122	0.165	0.184	0.103
SR	3.55	4.3	3.64	3.94	3.3	3.58	4.53	4.1
T (°C) pour $G' = G''$	17	28	29	31	24	26	34	25
T (°C) pour G'' max	−10	−10	0	−5	0	−5	−15	−10
δδ (−10°C; 5 Hz)	12.2	11.6	7	9.1	6.5	8.3	12.7	11

NOTE: SR = standard deviation of the relaxation spectrum.

It should be noted that this hard binder is not available in all locations (Denneman et al., 2011) and might require innovative binder modification techniques to achieve the desired results. When Korea experimented with HMAC, they mixed a high boiling point petroleum with a conventional asphalt to increase binder stiffness. At that point, 4% styrene-butadiene-styrene was introduced so that the binder could maintain some ductility. Despite the addition of polymer, the binder developed for the HMAC was still more brittle at low temperatures than conventional or polymer-modified asphalt when determining Frass temperature (Lee et al., 2007). Thermal distress is not common in many European countries; however, this becomes a more critical property to monitor as HMAC is adopted in countries with colder climates (EAPA, 2005).

Today, polymer-modified asphalts (PMA) are part of the available binder selection for HMAC. Polymer-modified asphalts resist rutting in summer months and provide flexibility to resist tensile stresses. Some research suggests that even the incorporation of fibers as part of the PMA can provide additional durability to reduce cracking; however, additional information is needed to ensure these findings (Montanelli, 2013).

A similar experiment to the Korean study was conducted in Lithuania that compared HMAC with crushed granite, crushed dolomite, and crushed gravel. Additionally, two polymer-modified binders and a traditional HMAC hard binder were used to give the study nine mixture iterations. Mixtures were designed and tested for stiffness modulus (LST EN 12697-26), resistance to rutting (LST EN 12697-22), fatigue resistance four-point bending (LST EN 12697-24), and stability and flow (LST EN 12697-34). While some differences were seen between aggregate types, the type and amount of binder made the most difference. The study recommended that polymer-modified binders be recommended for HMAC base mixtures and only polymer-modified binders be used in the binder layers. This recommendation was based off of fatigue results, which showed that the mixtures with polymer-modified binders (PMB) performed better than those without polymer (Vaitkus, 2013).

Chappat et al., (2009) proposed similar findings that binder source is a crucial component of producing a high performing HMAC. When comparing modulus values to fatigue strength for mixtures using different binder sources, the research team could see tendencies for some binders to outperform others. For example, in Figure 2, one sees that from source A, the mixture will get the modulus but have trouble attaining the fatigue requirements. On the other hand, source B

produces mixtures that are too soft but have adequate fatigue performance. Knowing the materials is vital for producing mixtures that will be judged on performance.
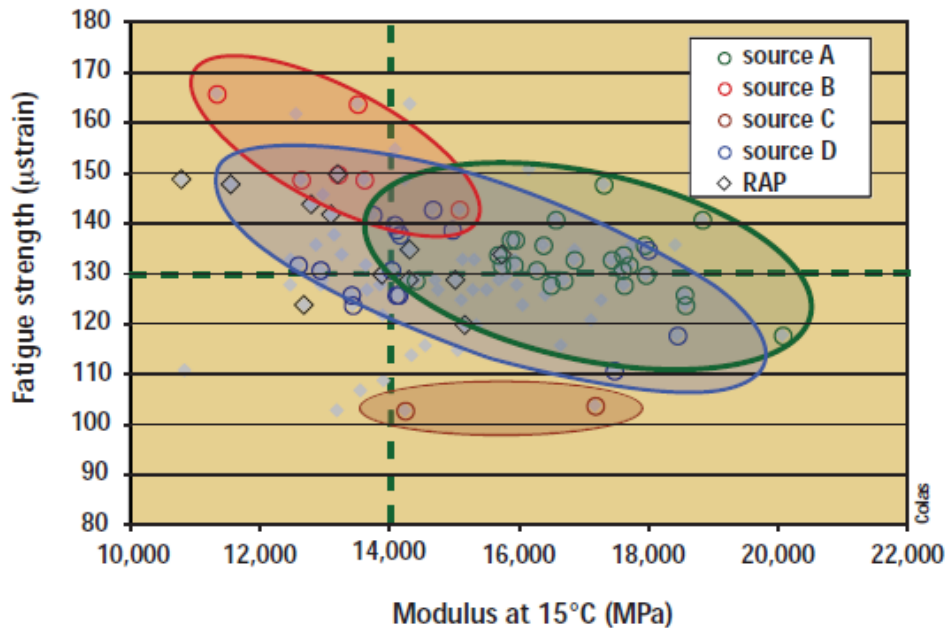
Figure 2 Combined Presentation of the Modulus and Fatigue Strength Results According to Binder Source (Chappat et al., 2009)

Increased binder rigidity is commonly balanced by using higher binder contents in the mixtures (Guyot, 2013). Minimum binder contents are given based on the class of the mixture and the maximum aggregate size. The French have seen a continual increase in binder content and increased binder stiffness to help produce high-modulus mixtures since the 1970s (Figure 3) (Distin et al., 2006).
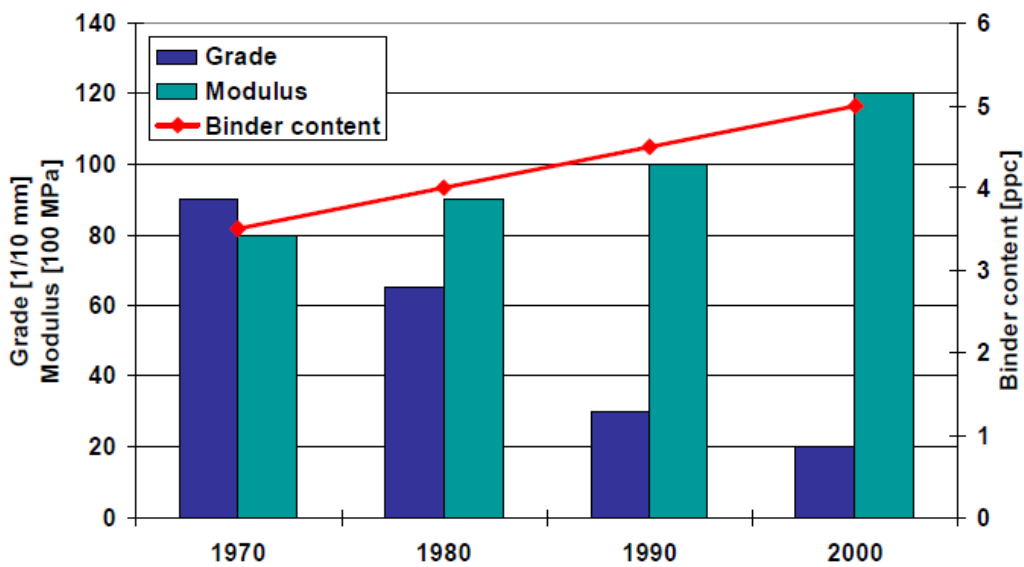
Figure 3 Evolution of Base Course Mixtures in France (Distin et al., 2006)

The Class 1 mixture is less fatigue resistant and designed for lower traffic volumes while the Class 2 mixture is designed for higher volumes with additional resistance to fatigue. Table 6 provides the minimum binder contents based on aggregate density (ρ), class, and maximum aggregate size. Binder content is calculated not through volumetric properties like in the U.S., but by calculating a richness factor, K. However, the Asphalt Institute binder film thickness equation seems better because is based on the actual measure of asphalt absorption; ie effective binder film thickness. This factor is calculated through the following method (Denneman et al., 2011; Denneman and Nkagdme 2011).

1. Calculate the specific surface area of the aggregate (Σ) using Equation 1.

$$100\Sigma = 0.25G + 2.3S + 12s + 150f \tag{1}$$

where

G = proportion of aggregate retained on and above the 6.3 mm sieve;
S = proportion of aggregate retained between the 0.25 mm and 6.3 mm sieves;
s = proportion of aggregate retained between the 0.063 and 0.25 mm sieves; and
f = percent passing the 0.063 mm sieve.

2. Calculate a correction coefficient (α) for the relative density of the aggregate (RDA) using Equation 2 (in this case RDA = Gse).

$$\alpha = \frac{2.65}{RDA} \tag{2}$$

3. Calculate the binder content of the mixture by mass of total aggregate using Equation 3.

$$TL_{est} = K\alpha\sqrt[5]{\Sigma} \tag{3}$$

4. Calculate the percent binder by mass of total mixture using Equation 4.

$$TL_{est} = \frac{100P_b}{(100-P_b)} \tag{4}$$

Table 6 Typical Values for Minimum Binder Content and Target Richness Factor (Denneman et al., 2011)

|	HMAC Base Course		
	Class 1	Class 2	
D (mm)	10, 14, 20	10, 14	20
$P_{b\,min}$ ρ=2.65 g/cm^3	3.8	5.1	5.0
$P_{b\,min}$ ρ=2.75 g/cm^3	3.8	4.9	4.9
Richness factor, K	2.5	3.4	3.4

3.1.4   Performance Tests

Once the binder content is determined, the final phase of mixture design is to undergo a series of performance tests to ensure the mixture will be durable in the field. The French suite of tests revolves around five standards (Table 7).

Table 7 French Performance Tests (Modified from Denneman et al., 2011)

Parameter	French Test Method
Workability	EN 12697-31: Gyratory Compactor
Durability	EN 12697-12: Duriez test
Permanent Deformation	EN 12697-12: Wheel Tracker
Dynamic Modulus	EN 12697-26: Flexural beam
Fatigue test	EN 12697-24: Prism

The workability of the asphalt mixtures is assessed by ensuring that the mixture has less than the maximum void content after 100 gyrations in the European gyratory compactor. South Africa conducted a study using the Superpave gyratory compactor to assess what deviations occur when switching from testing using the European standard to the Superpave method. The study showed that the equivalent gyrations and average air voids were reduced for the Superpave method (Figure 4 and Table 8).
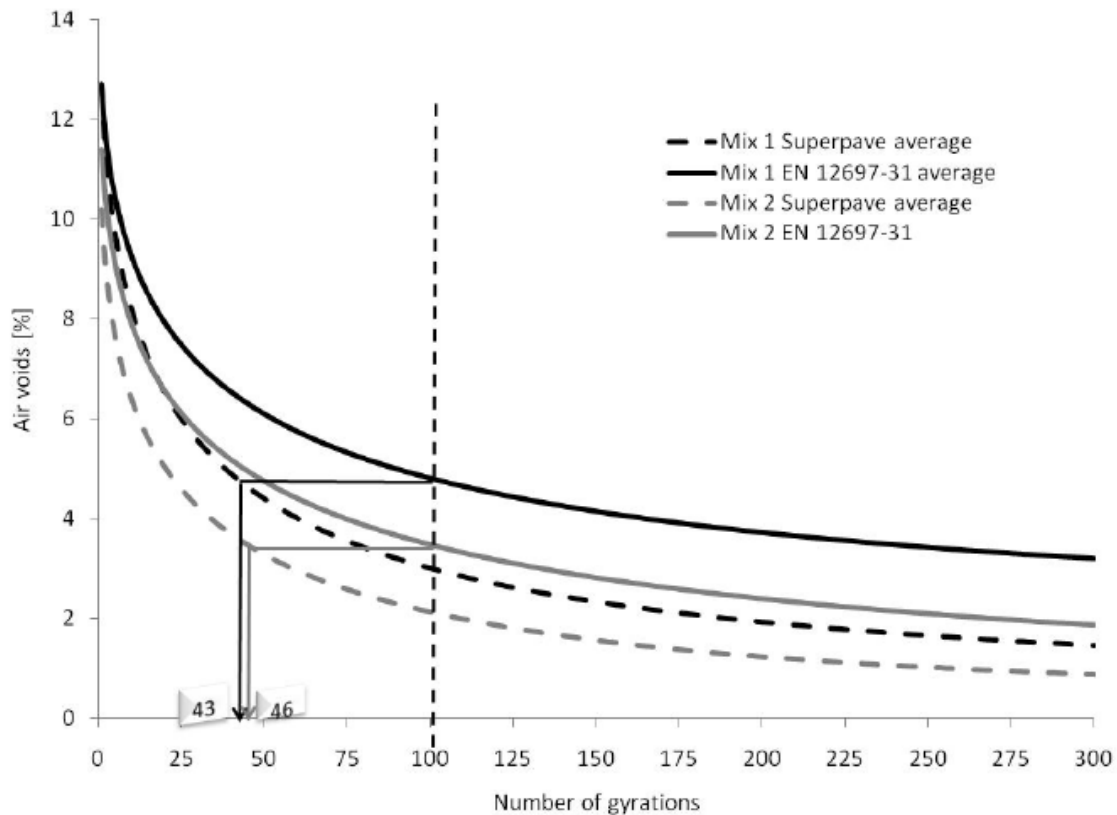
Figure 4 Gyratory Compaction Curves for Two Mixtures using European and Superpave Configuration (Denneman et al., 2011)

Table 8 Summary of Gyratory Compaction Study (Denneman et al., 2011)

HMAC Design	Class 1		Class 2	
Specification	EN 12697-31	Superpave	EN 12697-31	Superpave
Number of Specimens	9	8	5	5
Average Voids (%) after 100 Gyrations	4.8	3.0	3.5	2.2
Standard Deviation	0.8	0.9	0.8	0.4
Coefficient of Variation (%)	16.0	30.0	22.1	19.8
Equivalent Gyrations	100	43	100	46

The Duriez test is the French equivalent of AASHTO T283 for moisture susceptibility. In South Africa, a modified Lotmann test (ASTM D4867) is used to assess durability. Most countries that use HMAC do not differentiate tensile strength ratio (TSR) requirements between asphalt mixtures and HMAC (Denneman et al., 2011).

EN 12697-22 is the standard in Europe for assessing rutting resistance of mixtures by wheel tracking on an asphalt slab. The wheel tracking apparatus consists of a loaded wheel, which bears on a sample held on a moving table. The table reciprocates with simple harmonic motion through a distance of 230 ± 5 mm with a frequency of 53 passes (± 1%) per minute. For research purposes, the test speed can be adjusted by inverter control. The wheel is fitted with a solid rubber tire of outside diameter 200 mm. The wheel load under standard conditions is 700 ± 10 N. The wheel tracker is fitted with a temperature controlled cabinet with a temperature range from environment to 65°C ± 1.0°C. The sample may be either a 200 mm diameter core or a 300 x 400 mm slab of asphaltic mixture from 25mm to 100 mm thick. A 25 mm stroke LVDT transducer is included for monitoring rut depth in the center of a sample during a test to better than 0.1 mm. The deformation and sample temperature is recorded by the internal data acquisition and control system and is then sent to the Windows® compatible software.

Other countries use their own standard rutting tests such as AASHTO T320, the Repeated Simple Shear Test at a Constant Height. Research has consistently shown that despite the higher asphalt content in HMAC, the stiffer binder allows the mixture to resist rutting more than a standard bituminous base material (BTB) (Figure 5) (Denneman et al., 2011). This is an especially important consideration in warmer climates due to the extra binder, which adds to the richness of the mixture (Capitão and Picado-Santos, 2006).
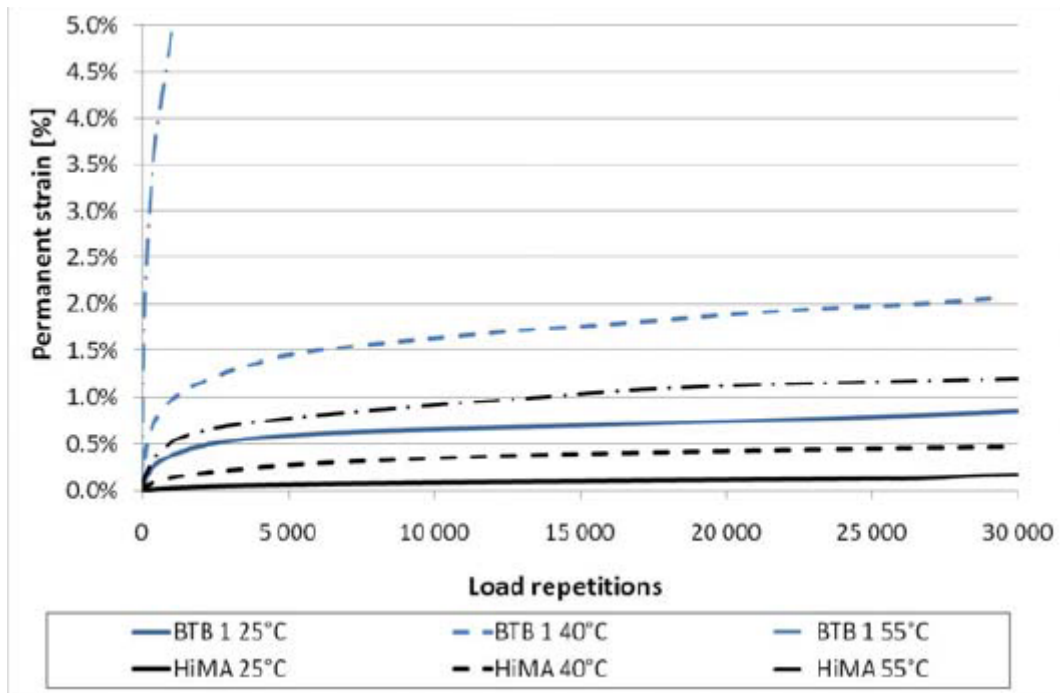
Figure 5 Permanent Deformation HMAC Compared to BTB (Denneman et al., 2011)

In Europe, dynamic modulus is measured using standard EN 12697-26 (equivalent to AASHTO TP 62) where the stiffness of the asphalt mixture beam is determined (AASHTO T321). HMAC must then have a stiffness greater than 14,000 MPa at 10°C and a frequency of 10 Hz. While just ensuring that the mixture can surpass this stiffness at one temperature provides an easy check, it limits the data available to the practitioner. Additionally, choosing 10°C might be an appropriate check in the temperate climates of Europe; however, other countries such as South Africa have decided to use a higher temperature of 15°C and still require a stiffness greater than 14,000 MPa due to hotter climates. South Africa has also implemented AASHTO TP 62 as the method for ascertaining mixture stiffness, which is more comparable to what might be done if HMAC was to become a design methodology in the U.S. (Denneman et al., 2011). While choosing one temperature and frequency to check the stiffness, Figure 6 shows that HMAC (EME) mixtures are typically stiffer than conventional mixtures across the temperature-frequency spectrum (Petho and Denneman, 2013).
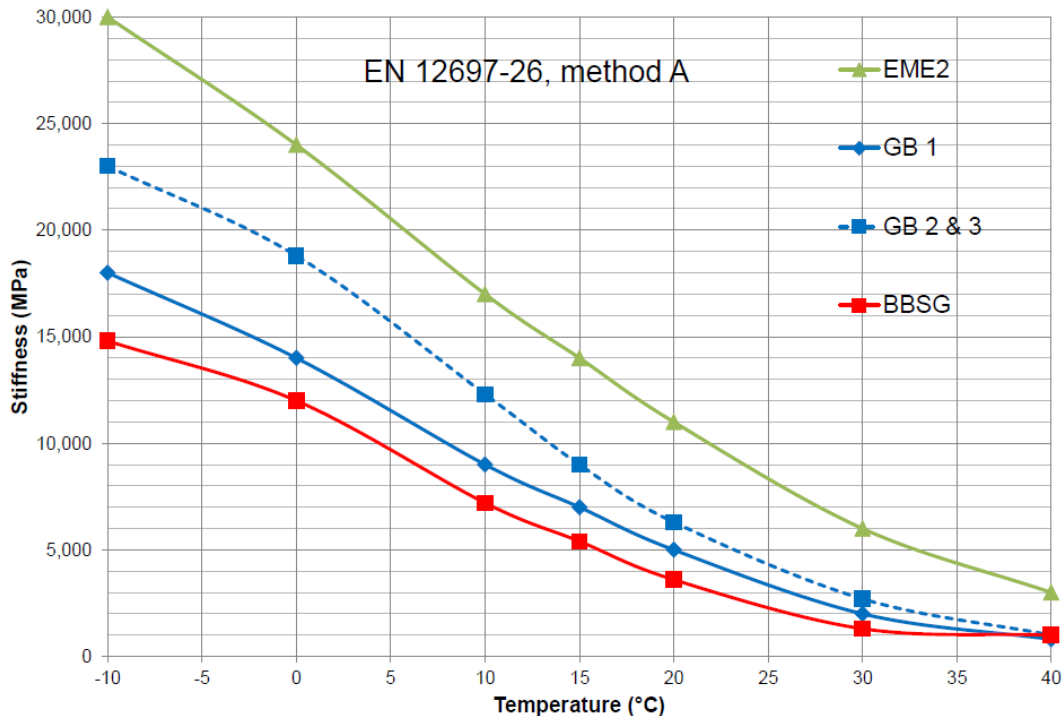
Figure 6 Dynamic Modulus of High-Modulus Compared to Common European Mixtures (Petho and Denneman, 2013)

The final performance test for HMAC mixtures is fatigue. While the mixture is stiffer, it is still important for it to retain some elasticity and resistance to fatigue cracking. The Europeans test fatigue through the bending of a prism, which is not common in the United States. South Africa uses a four-point bending fatigue test on beams following AASHTO T321. South African tentative performance criteria require Class 1 mixtures to have no greater than a 70% stiffness reduction at 310 microstrain for 10,000,000 repetitions. For a Class 2 mixture, this requirement is set for a strain load of 410 microstrain (Denneman et al., 2011).

Some concerns have been raised about fatigue test repeatability and results. A laboratory and full scale pavement testing study was conducted at Nantes, France to assess four different mixtures' behaviors to fatigue in various laboratory and field conditions. The circular test track of LCPC used four different mixtures to make up each quadrant of the track: (1) an asphalt mixture with 50/70 pen asphalt from one source, (2) an asphalt mixture with 50/70 pen asphalt from a second source, (3) an HMAC with 10/20 pen asphalt, and (4) a road base asphalt with 50/70 pen asphalt. In addition to the field work, each mixture was subjected to fatigue testing using the following procedures: (1) two-point bending fatigue tests on trapezoidal samples with controlled strain, with and without rest periods; (2) two-point bending fatigue tests on trapezoidal samples with controlled stress, without rest periods; and (3) three-point bending fatigue tests on parallelepiped-like samples, with control stress, with and without rest periods.

The laboratory rankings of the materials depended greatly on the testing procedure, showing that choosing the correct testing protocol is critical for ensuring that the right mixture properties

are being analyzed. However, for the field experiment, 1.0 cm of very thin asphalt concrete (VTAC) was placed over 7.7 cm of HMAC, and it was compared to 1.5 cm of VTAC over 10 cm of road base asphalt. All asphalt materials were placed over a softer base than is typically found in France. The study used a 65 kN dual wheel at 10 rpms (70 kph linear due to 19 m radius of testing device) to load the pavements for 2,665,000 load repetitions. Figure 7 shows less deflections in the typical road base (GB3) compared to the HMAC (EME) mixtures; however, the authors also note this was not the typical condition for EME mixtures due to the softer subgrade. As for cracking, the HMAC was the last mixture to exhibit fatigue cracking; however, once it exhibited cracking, it tended to progress faster, showing the more brittle nature of the material (Figure 8). It should be noted that these experiments were conducted before polymers were commonly used in HMAC binders (de La Roche et al., 1994).
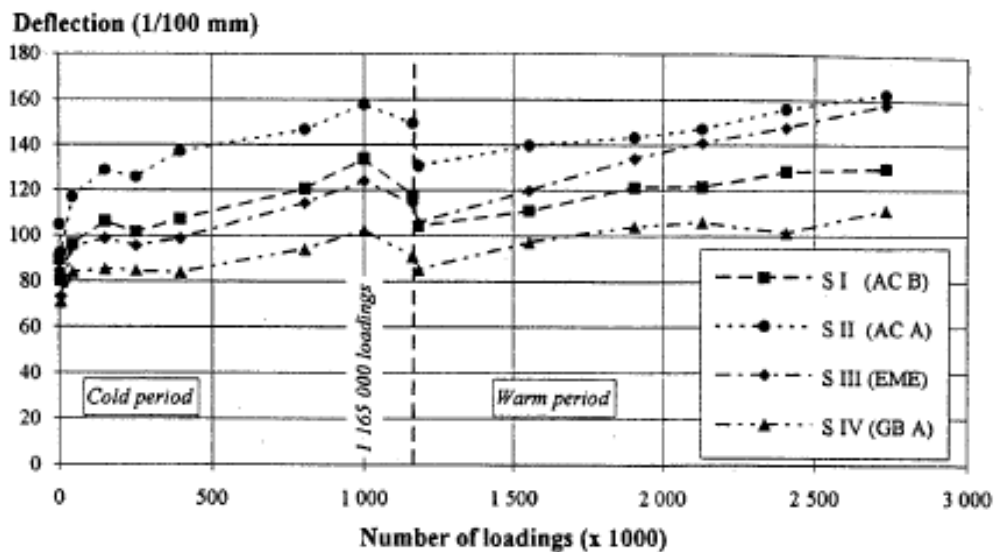
Deflections 1/100 mm (20°C)	Number of loadings	Sector I AC B	Sector II AC A	Sector III EME	Sector IV GB A
	40,000	96	117	95	84
	1,165,000	118	150	114	91
	2,700,000	129	163	158	111

Figure 7 Deflections Referred to 20°C (de La Roche et al., 1994)
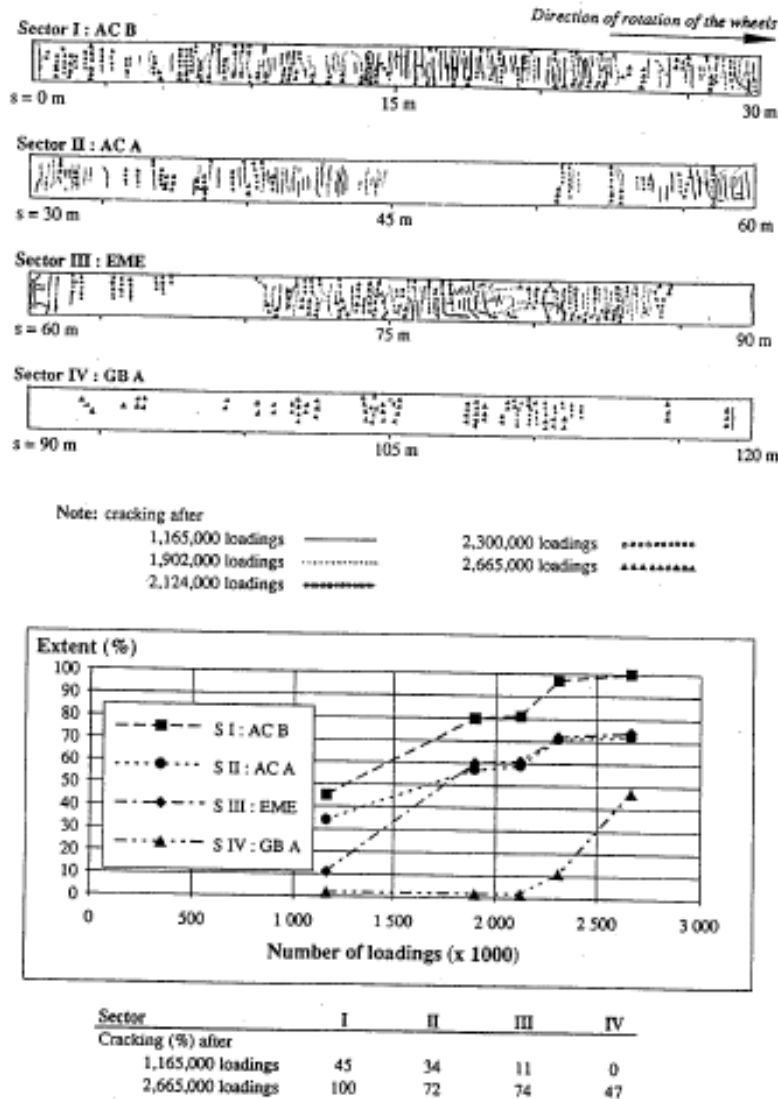
20

Figure 8 Cracking (de La Roche et al., 1994)

3.2   Pavement Design

The National Asphalt Pavement Association recognized the potential for HMAC to be an integral part of long-life or perpetual pavement design. The organization recognized early that the French had used HMAC to justify thinner sections for their long-life pavement designs (Newcomb and Hansen, 2004; Newcomb et al., 2010).

The French have developed an analytical pavement design method that can capture the effects of HMAC. LCPC has developed Alize-LCPC software, which uses a mechanistic-empirical approach where traffic, material properties, and performance coefficients are used to predict pavement performance (Guyot, 2013), but other design programs can be used that incorporate material properties into design.

One case study that incorporated HMAC as a design option was the 2011-12 runway overlay and new parallel taxiway at the Sir Seewoosagur Ramgoolam International Airport in Mauritius in the Indian Ocean. When comparing the typical runway buildup from the FAARFIELD Airport Pavement Design Software sponsored by the FAA, the use of HMAC reduced the necessary runway thickness by 105 mm. Not only did this save money and natural resources, but a study showed that it also saved approximately 13% in greenhouse gas emissions (Guyot, 2013).

As Thailand was considering using HMAC in pavement structures, Alize-LCPC was used to conduct structural analyses given an expected modulus of 14,000 MPa and fatigue resistance (10^6 cycles) at 130 microstrain for the HMAC. The road base asphalt was expected to have a modulus of 9,300 MPa and a fatigue resistance (10^6 cycles) at 90 microstrain. The design software showed that for similar wearing courses, 7 cm less structure was needed for the HMAC mixtures, thus, reducing the required pavement structure by 20% (Lefant, 2012). Other sources cite that some governments have seen a 30% reduction in needed pavement structure due to the increased stiffness of the pavement and added fatigue resistance (Corte, 2003).

Carbonneau et al. (2008) conducted an experiment where they compared the reference cross-section of the Herning bypass to two cross-sections containing HMAC mixtures, called a HMA GAB II mixture in Denmark. When the mechanical properties of the two mixtures were placed through a mechanistic-design program, the use of the HMAC mixture allowed the bypass cross-section to be reduced by 25 mm in thickness. The two final cross-sections are given in Figure 9. This analysis resulted in the HMAC mixture being used to reduce material quantities, and the roadway is currently being monitored (Carbonneau et al., 2008).
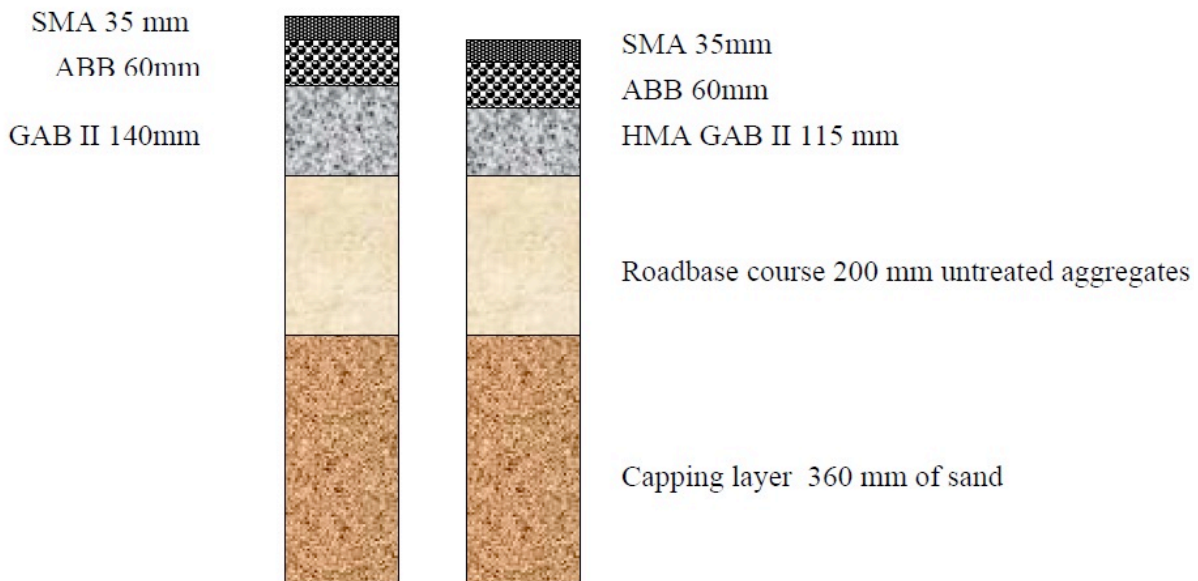
Figure 9 Roadway Structure of Mixture Design Based on Characteristic Mechanical Gain of HMA GAB II (Carbonneau et al., 2008)

Weilinski and Huber (2011) showed these mixtures could be incorporated into the current version of the Mechanistic-Empirical Pavement Design Guide (MEPDG). The design incorporated American materials from Indiana that included recycled asphalt shingles (RAS), RAP, binder, and aggregate. The team found that binder stiffness had little to do with performance in the MEPDG on rutting, IRI, or fatigue cracking. These results were similar when comparing stiff mastercurves like the PG 64-22 binder with RAS compared to the PG 76-22 binder mastercurve. The increased mixture stiffness did improve fatigue performance and ride in the MEPDG. Additionally, using the HMAC reduced the pavement thickness by 16% to achieve similar performance.

3.3   Performance

A small-scale laboratory experiment was conducted in China to assess the impact of high-modulus asphalt on rutting resistance when compared to polymer-modified and conventional softer binders when used in the binder course of a pavement. Using finite element modeling, the shear strains and compressive stresses within the middle of the pavement were calculated through a typical pavement cross-section for the area. The results (Figure 10) show that using the high-modulus materials reduced shear strain. These results also showed that despite the higher binder content used in an HMAC design, the rutting resistance of the pavements using the HMAC was increased (Wei et al., 2010).
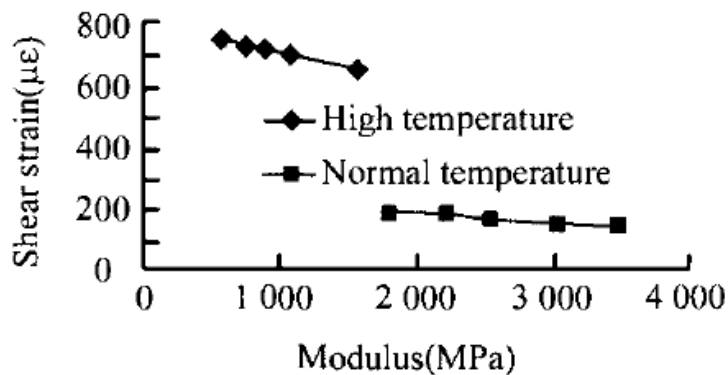

Figure 10 Tendency of Shear Strain (Wei et al., 2010)

A field experiment was developed outside of Brussels, Belgium to assess how aggregate skeleton, recycled materials, binder content, and grade all influenced field performance of pavement structures with HMAC binder courses. Each 140-m test section was constructed with a 9 cm variant of an HMAC with a 3 cm stone matrix asphalt (SMA) or porous asphalt surface. During construction, cores were taken from each test section and tested for rutting using EN 12697-22 at 50°C. The results (except for the porous asphalt sections) showed that using HMAC improved rutting resistance. The differences in aggregate skeleton (stony versus sandy) did not impact the rutting values of the mixtures, nor did binder type. The primary driver for rutting resistance was binder content, as mixtures with lower binder contents had less rutting (Figure 11). After a year in the field, the high-modulus test sections all out-performed the control test section (DeBacker et al, 2008; DeBacker, deVisscher et al., 2008).
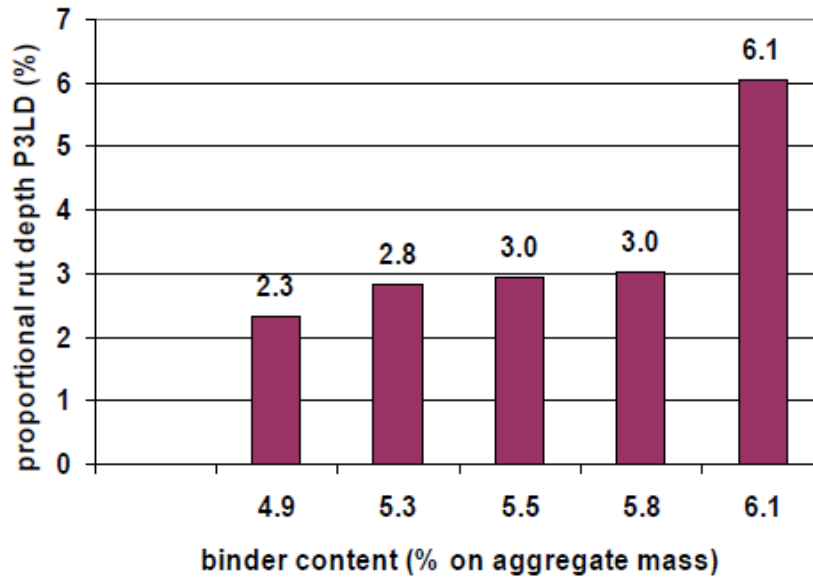
Figure 11 Rut Depth as a Function of Binder Content for Mixture with Sand Skeleton (deVisscher et al., 2008)

The country of Korea wanted to evaluate the use of HMAC for long-life pavements. After developing an HMAC mixture design, the HMAC was compared to a conventional asphalt mixture in performance tests before being introduced at an accelerated loading facility. The mixtures were evaluated for stiffness (Figure 12), fatigue in indirect tension (Figure 13), rutting via KS F2374 test procedure, and moisture damage using ASTM D4867 (Table 9). In all cases, the HMAC was shown to perform better than the conventional mixture.
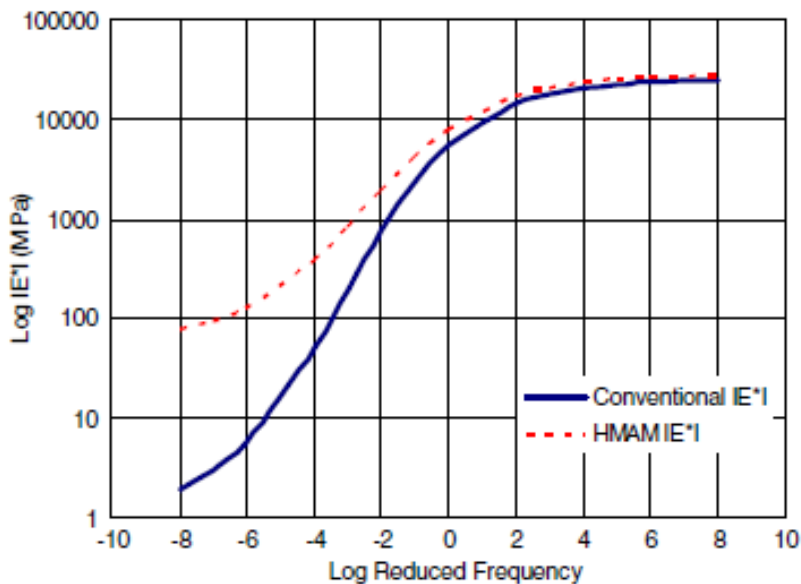
Figure 12 Dynamic Modulus Mastercurves at 15°C Reference Temperature (Lee et al., 2007)
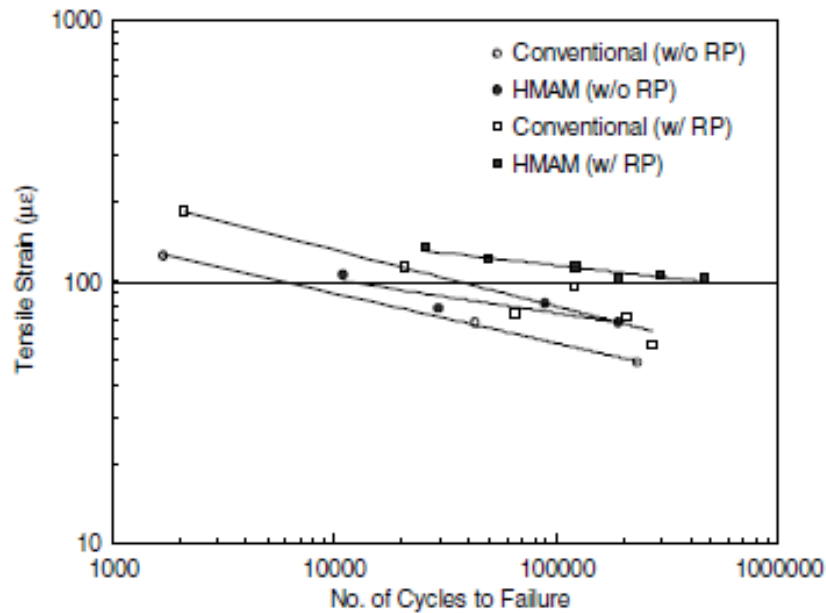
*RP = rest period

Figure 13 Results of Fatigue for the Conventional Mixture and HMAC (HMAM) (Lee et al., 2007)

Table 9 Performance Test Results from Korean Laboratory Study (Data from Lee et al., 2007)

Mixture	Dry Strength, kPa	Wet Strength, kPa	TSR	Rut Depth, mm
Conventional	1070.9	948.3	88.54	7.28
HMAC	1515.1	1489.6	98.32	2.79

Due to the success in the laboratory, these mixtures were then compared in the field at the Hanyang University Accelerated Pavement Tester. In this procedure, an 11-ton load (maximum axle load in Korea is 10 tons) is applied to 12.5 m of pavement at a maximum speed of 17 km/h. Two lanes of these mixtures were produced. The first lane was designed to study fatigue cracking and the experimental mixtures were constructed at 94 and 83 mm in thickness for the conventional and HMAC mixtures, respectively. The second lane was designed to study rutting and the mixtures were constructed thicker. The conventional mixture was 268 mm thick while the HMAC mixture was 215 mm thick. Strain gauges were placed at the bottom of the asphalt layer to characterize the pavement response.

The results showed that despite having a thinner cross-section, the HMAC could reduce the tensile strains in the test sections except for the thin test section at the lowest wheel loading (Figure 14). The preliminary results suggested that this fatigue performance would, in fact, allow Korea to use these mixtures as part of a long-life pavement concept with additional validation as no fatigue cracking was noticed in either test section at the end of the experiment. The high-modulus mixtures also performed better than the conventional mixtures in terms of rutting

(Figure 15). The HMAC mixture had less than half of the rutting in the conventional mixture despite being constructed on a thinner asphalt cross-section (Lee et al., 2007).
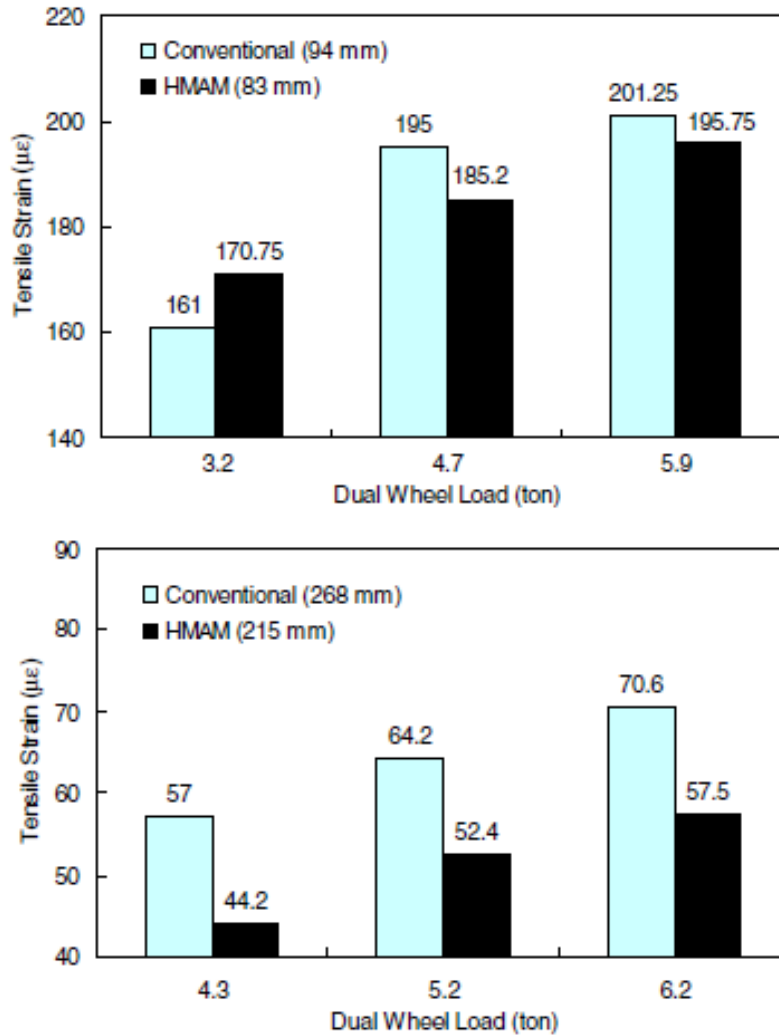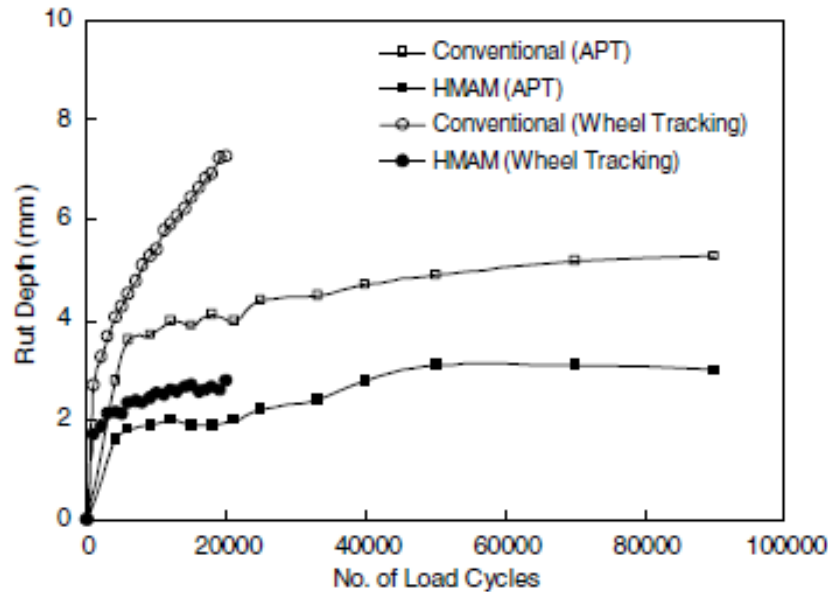

Figure 14 Tensile Strain with Change of Dual Wheel Load for (a) Thin Pavement Section and (b) Thick Pavement Section (Lee et al., 2007)

Figure 15 Comparison of Rut Depths for Conventional Mixtures and HMAC Pavement (Lee et al., 2007)

As part of the implementation effort in Europe, two HMAC mixtures were compared to two basic asphalt mixture designs in the laboratory and the field. Field testing was conducted under a heavy vehicle simulator (HVS). Structural cross-sections of the four test sections are provided in Table 10. The HVS applied 60 kN via a single axle loading with a tire pressure of 800 kPa at a speed ranging from 10-12 kph.

Table 10 Structural Build-Ups (Information from Barkowski et al., 2007)

Pavement Layer	A	B	C	D
Wearing Course	Thickness: 2 cm Mixture type: SMA Binder: PmB 45/8065		Thickness: 4 cm Mixture type: porous Binder: 50/70	Thickness: 4 cm Mixture type: SMA Binder: PmB 45/80-65
Binder Course	Thickness: 10 cm Mixture type: HMAC 16 Binder: 20/30	Thickness: 10 cm Mixture type: AC 16W Binder: 35/50	Thickness: 8 cm Mixture type: AC 16W Binder: 35/50	Thickness: 7 cm Mixture type: HMAC 15 Binder: 20/30
Unbound Materials	Thickness: 20 cm Aggregate: dolomite			

Additionally, modeled fatigue life and damage were determined based on the Asphalt Institute transfer function considering a 60 kN with the HVS wheel configuration. The two HMAC test sections showed the best performance (Figure 16). It is interesting to note that section D had higher measured and modeled strains than Section A (Figure 17); however, it had better expected

27

performance. This may have been due to the differences in fatigue performance of the HMAC in the binder/base course (Bankowski et al., 2009).

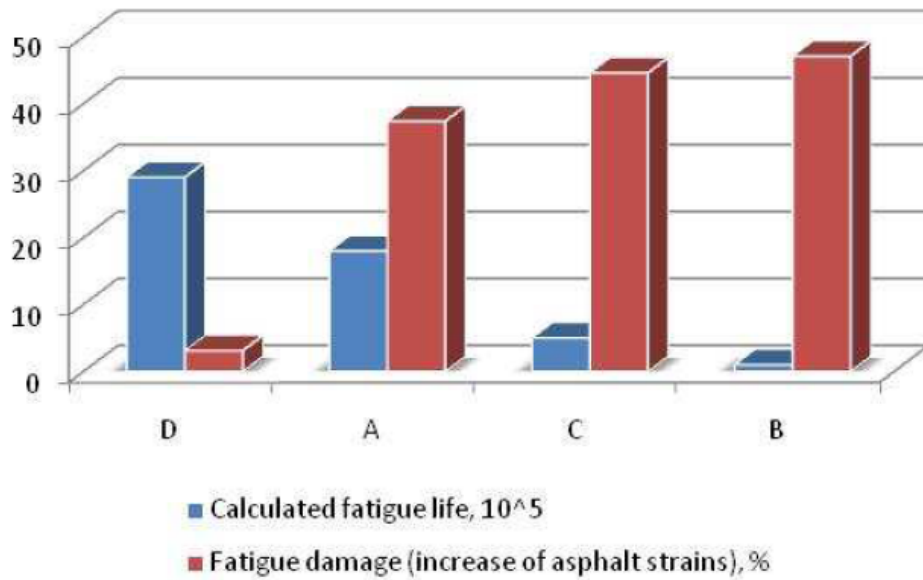**Figure 16 Comparison of Fatigue Life for Each Individual Section (Bankowski et al., 2009)**
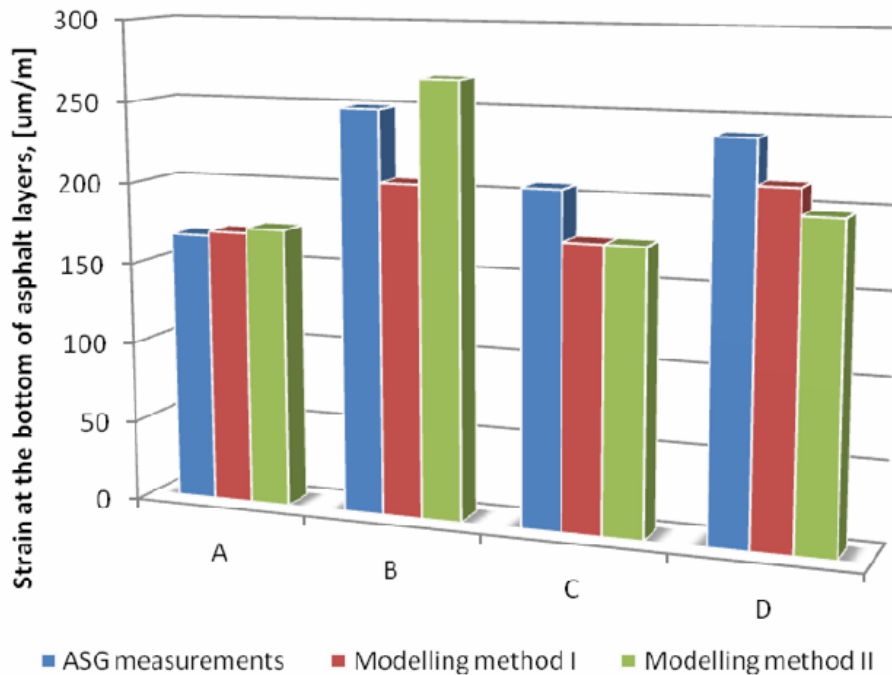

Figure 17 Comparison of Measured and Calculated Strains at the Bottom of the Asphalt Layers (Bankowski et al., 2009)

In 2010, the Virginia Transportation Research Council (VTRC) reported the results of a study of field trials of high-modulus high-binder-content base layer hot-mix asphalt mixtures

(Diefenderfer and Maupin, 2010). Three locations where deep rehabilitation or new construction were selected, and HMA base mixtures were used at designed asphalt content, designed asphalt content plus 0.4% additional asphalt, and/or designed asphalt content plus 0.8% additional asphalt. Two of the field trial locations had no construction-related issues; difficulties during compaction occurred at the third. The results of this study indicated that the binder stiffness for an HMAC mixture should be at least equivalent to that of a PG 70-22 binder to guard against potential rutting and addition of RAP may be necessary.

3.4   Construction

While little has been published regarding the construction of these mixtures, the Belgian study did gain some insights to the approach. At times, conventional methods were not appropriate either due to the design asphalt content or binder stiffness; thus, the research team made note of the following items: (1) contractors must use binder producer's recommended temperatures during production; (2) common aggregate size to lift thickness ratios did not apply, as HMAC was placed 9 to 10 cm thick without any problem; (3) mixtures were easy to compact with traditional equipment; (4) compaction temperatures were commonly about 10°C higher than conventional mixtures; (5) the fatty look of the mixture does not indicate over compaction; and (6) voids ratios were similar to those in conventional binder courses (DeBacker et al., 2008). Denneman (2011) observed that these mixtures commonly require higher mixing temperatures.

Nicholls et al. (2008) conducted an experiment to monitor the durability and buildability of HMAC on five different sites in the UK. During the pilot projects, some instances were noted when the level of compaction was not achieved (Site D); however, on other trial projects, the in-place air voids were extremely low (1% at site B). Falling weight deflectometer and laboratory tests showed that with few exceptions, the mixtures were designed, produced, and constructed well.

Michaut (2014) provided the following recommendations for producing and laying HMAC:

- Mixing temperature should be between 160 and 180°C and always less than 190°C.
- The minimal laying temperature for this mixture is 145°C, but this will depend on binder properties.
- Granular base must be compacted well to ensure high in-situ density of HMAC.

Jamois et al. (2000) notes that sometimes these temperatures can be exceeded if material properties dictate the need. Mixtures placed at the circular test track in France were produced between 200 and 210 °C and placed at 195°C.

3.5   Summary of Current Practice

A comprehensive literature study was performed to assess the current state-of-the-practice on HMAC mixture design, pavement design, laboratory performance tests, and full scale pavement performance. The majority of the observed experience comes from Europe. The French HMA mixture design method is the most commonly used methodology and has some variations in the design procedure compared to conventional Superpave design mixtures commonly utilized in the

United States. The first main difference is the method of compaction. The determination of minimum binder content in the French design method is also quite different from Superpave design. The French method calls for a minimum asphalt binder content based on the richness factor, surface area, and specific gravity of the aggregates. However, as mentioned before, the AI Hveem-Edward binder film thickness calculation is as good. Asphalt mixture design procedures include performance testing requirements for moisture damage, a rut test for rutting, complex modulus for structural stiffness, and fatigue testing for fatigue cracking.

Pavement design and analysis of HMAC mixtures is conducted using mechanistic-empirical approaches. This practice includes evaluation of potential field performance and reduction in needed pavement structure due to the increased stiffness of the pavement and added fatigue resistance. Full scale performance testing has been used to validate this added fatigue resistance.

Overall, there is an expected difference in the laboratory performance of HMAC mixtures when compared to traditional asphalt mixtures. This performance difference is expected to translate into the field where pavements can either be designed thinner with the same expected life or designed at the same thickness with long-life performance as a viable expectation. Table 11 exhibits an example of change in specifications for HMAC mixtures compared to conventional asphalt concrete mixtures in Europe.

Table 11 Roadbase High-Modulus Asphalt Concrete versus Traditional AC (EAPA, 2005)

Roadbase High-Modulus Asphalt Concrete versus Traditional AC			
Test	HMACR1	HMACR2	AC
Inmersion Copression test at 18°C	>0.7	>0.75	>0.7
Rutting test at 60°C 30,000 cycles	<8%	<8%	<10%
Stiffness modulus at 15°C and 10Hz	>14,000 MPa	>14,000 MPa	>9,000 MPa
Allowed microstrain from fatigue law at 10°C and 25 Hz and for 10^6 cycles	>100	>130	>90
Void content for laying thickness	<10%	<6%	<10%

4.   EXPERIMENTAL DESIGN AND ANALYSIS

4.1   Laboratory Testing

There were two objectives addressed in the laboratory experimental plan: (1) determine the engineering properties of high-modulus mixtures, and (2) determine whether or not the recommended design procedures were appropriate. The information to accomplish both objectives was obtained from European experience. This section details the approach adopted to address the two objectives of the laboratory research.

To assess statistical differences among mixtures, the general linear model (GLM) ($\alpha = 0.05$) was conducted. Overall comparisons of such properties were made using Tukey-Kramer analysis with the results from all laboratory performance tests. The results of the laboratory testing were also used to determine if the current testing procedures could adequately predict the performance

of pavements containing these types of mixtures in the field. The laboratory testing program evaluated binder performance grade, mixture stiffness over a wide temperature range, fatigue cracking, and permanent deformation, as follows:

- Volumetric mixture design and material characterization,
- Mixture stiffness: dynamic modulus (AASHTO TP 79-13),
- Flow number (AASHTO TP 79-13), and
- AMPT cyclic fatigue (AASHTO TP 107-14).

4.2   Mixture Design

The French asphalt mixture design method has some variations in the design procedure compared to conventional Superpave design mixtures commonly utilized in the United States. The French gyratory compactor uses an internal angle of 0.82 degrees, whereas the Superpave gyratory compactor employs an internal angle of 1.16°. Wielinski and Huber (2011) used in their research study the results of a comparison study of the LCPC gyratory compactor and a Superpave gyratory compactor for EME mixture design that was conducted by the Jiangsu Transportation Research Institute. This comparison work determined that 80 gyrations in the Superpave compactor produced the same compaction as 100 gyrations in the LCPC gyratory compactor.

For this study, samples were compacted at 80 gyrations in the Superpave compactor, and the target design air voids at N_{des} was set from 3.0 to 6.0% (European specification requires design air voids to be less than six percent). For dynamic modulus testing, the range of allowable air void content was also 3.0 to 6.0% with a minimum dynamic modulus at 15 °C and 10 Hz of 14,000 MPa. In addition, the gradation selected for each trial dictated the minimum binder content required in the design according to the French methodology.

The experimental plan included a variety of mixtures with different material and binders such that higher moduli were obtained compare to conventional mixtures. The plan included a French mixture with a stiff binder (PG 88-16), two mixtures containing 35% RAP both with polymer-modified binders, but one high polymer content (HiMA), another mixture containing 25% RAP and 5% RAS with a polymer-modified binder, and finally, a 50% RAP mixture with a polymer-modified binder.

Table 12 shows the aggregate gradations and blend formulas for the four mixtures that were produced. Table 13 shows the volumetric properties of each mixture determined during the design phase.

Table 12 Aggregate Gradations of Mixtures

Sieve Size (in.)	French EME 14	35% RAP PG 76-22	25% RAP, 5% RAS PG 76-22	35% RAP HiMA	50% RAP PG 76-22
2"	100.0	100.0	100.0	100.0	100.0
1.5"	100.0	100.0	100.0	100.0	100.0
1"	100.0	99.3	98.6	99.3	98.8
3/4"	100.0	95.5	91.0	95.5	92.4
1/2"	88.9	89.3	81.8	89.3	85.5
3/8"	79.7	79.5	72.6	79.5	78.5
#4	58.9	54.9	51.5	54.9	51.1
#8	37.7	42.7	41.5	42.7	40.7
#16	26.6	32.5	32.0	32.5	31.2
#30	19.3	22.5	21.5	22.5	21.3
#50	14.0	12.1	11.1	12.1	10.6
#100	8.8	7.1	6.4	7.1	5.9
#200	7.9	4.7	4.2	4.7	3.9

Table 13 Mixture Design Properties

Mixture Designation	French EME 14	35% RAP PG 76-22	25% RAP, 5% RAS PG 76-22	35% RAP HiMA	50% RAP PG 76-22
Gyration level	80	80	80	80	80
NMAS (U.S. sieves)	19	19	19	19	19
Binder content (%)	5.70	5.12	5.01	5.12	5.04
Base binder content (%)	5.70	3.24	2.73	3.24	2.98
Base binder grade	PG 88-16	PG 76-22 (SBS)	PG 76-22 (SBS)	PG 88-22 (High SBS)	PG 76-22 (SBS)
Percent RAP	0	35	25	35	50
Percent RAS	0	0	5	0	0
RAP AC%	n/a	5.37	5.37	5.37	4.12
RAS AC%	n/a	n/a	18.69	n/a	n/a
RAP binder ratio	n/a	0.367	0.268	0.367	0.409
RAS binder ratio	n/a	n/a	0.187	n/a	n/a
G_{sb}	2.751	2.716	2.730	2.716	2.690
G_{mm}	2.478	2.542	2.543	2.542	2.530
Design air voids (%)	1.5	2.0	3.0	2.3	2.6
G_{mb} design	2.441	2.491	2.467	2.484	2.464
VMA	15.0	13.0	14.2	13.2	13.0
VFA	90.0	84.6	78.8	82.6	80.0
G_b	1.028	1.028	1.028	1.028	1.028
G_{se}	2.709	2.761	2.757	2.761	2.743
P_{ba}	n/a	0.62	0.37	0.62	0.73
P_{be}	n/a	4.53	4.66	4.53	4.34
Dust proportion	n/a	1.03	0.91	1.03	0.90
E* at 15°C and 10 Hz, MPa	17,506	14,519	15,753	14,457	17,137
Air voids - E* specimen (%)	3.4	3.6	4.0	4.00	3.8

4.3 Dynamic Modulus

A single point measurement (E* at 15°C and 10 Hz) cannot be expected to describe material behavior across all possible loading temperatures/frequencies; therefore, Dynamic Modulus testing was performed for all mixtures according to AASHTO TP 79-13. In addition, these results were used to estimate pavement performance using the AASHTOWare Pavement ME Design software.

Samples were compacted to a height of 175 mm and a diameter of 150 mm and prepared to meet the tolerances outlined in AASHTO PP60-14. Dynamic modulus testing was performed in an IPC Global Asphalt Mixture Performance Tester (AMPT), shown in Figure 18. Dynamic modulus testing is performed in order to quantify the stiffness of the asphalt mixture over a wide range of testing temperatures and loading rates (or frequencies). The temperatures and frequencies used for testing these mixtures are those recommended by AASHTO PP61-13. For this methodology,

the high test temperature is dependent on the high PG grade of the base binder utilized in the mixture being tested.

Figure 18 IPC Global Asphalt Mixture Performance Tester

Dynamic modulus testing was performed in accordance with AASHTO TP 79-13 in an unconfined condition. Unconfined data is most commonly used for dynamic modulus testing since current mechanistic design software packages were calibrated using unconfined dynamic modulus data. Unconfined testing is also significantly easier to perform than confined testing and ME packages were calibrated using unconfined results.

The collected data were used to generate a mastercurve for each individual mixture. The mastercurve uses the principle of time-temperature superposition to horizontally shift data at multiple temperatures and frequencies to a reference temperature so that the stiffness data can be viewed without temperature as a variable. This method of analysis allows for visual relative comparisons to be made between multiple mixtures.

Generation of the mastercurve also allows for generation of the dynamic modulus data over the entire range of temperatures and frequencies required for mechanistic-empirical pavement design. By having an equation for the curve describing the stiffness behavior of the asphalt mix, both interpolated and extrapolated data points at various points along the curve can then be calculated. The general form of the mastercurve equation is shown as Equation 5. As mentioned, the dynamic modulus data are shifted to a reference temperature by converting testing frequency to a reduced frequency using the Arrhenius equation (Equation 6). Substituting Equation 6 into Equation 5 yields the final form of the mastercurve equation, shown as Equation 7. The shift factors required at each temperature are given in Equation 8. A reference temperature of 20°C was used for this analysis. The limiting maximum modulus in Equation 8 is calculated using the Hirsch Model, shown as Equation 9. The P_c term, Equation 10, is simply a

variable required for Equation 9. A limiting binder modulus of 1 GPa is assumed for this equation. Non-linear regression is then conducted using the 'Mastersolver.exe' program to develop the coefficients for the mastercurve equation. Typically, these curves have an S_e/S_y term of less than 0.05 and an R^2 value of greater than 0.99. Definitions for the variables in Equations 5 to 10 are given in Table 14.

$$Log|E^*| = \partial + \frac{(Max-\partial)}{1+e^{\beta+\gamma logfr}} \tag{5}$$

$$logf_r = log\,f + \frac{\Delta E_a}{19.14714}\left[\frac{1}{T}-\frac{1}{T_r}\right] \tag{6}$$

$$log|E^*| = \partial + \frac{(Max-\partial)}{1+e^{\beta+\gamma\left\{logf+\frac{\Delta E_a}{19.14714}\left[\frac{1}{T}-\frac{1}{T_r}\right]\right\}}} \tag{7}$$

$$log\,[a(T)] = \frac{\Delta E_a}{19.14714}\left[\frac{1}{T}-\frac{1}{T_r}\right] \tag{8}$$

$$|E^*|_{max} = P_c\left[4,200,000\left(1-\frac{VMA}{100}\right)+435,000\left(\frac{VFA*VMA}{10,000}\right)+\frac{1-P_c}{\frac{\left(1-\frac{VMA}{100}\right)}{4,200,000}+\frac{VMA}{435,000(VFA)}}\right] \tag{9}$$

$$P_c = \frac{\left(20+\frac{435,000(VFA)}{VMA}\right)^{0.58}}{650+\left(\frac{435,000(VFA)}{VMA}\right)^{0.58}} \tag{10}$$

Table 14 Mastercurve Equation Variable Descriptions

Variable	Definition
$|E^*|$	Dynamic modulus, psi
δ, β, and γ	Fitting parameters and parameters describing the shape of sigmoidal function
Max	Limiting maximum modulus, psi
f_r	Reduced frequency at the reference temperature, Hz
f	The loading frequency at the test temperature, Hz
ΔE_a	Activation energy (treated as a fitting parameter)
T	Test temperature, °K
T_r	Reference temperature, °K
a(T)	The shift factor at temperature, T
$|E^*|_{max}$	The limiting maximum HMA dynamic modulus, psi
VMA	Voids in mineral aggregate, %
VFA	Voids filled with asphalt, %

Figure 20 exhibits the mastercurves for all mixtures including the 19.0mm NMAS base course (control mixture) from the 2009 NCAT Test Track cycle. It can be observed that at the low temperature, high frequency end of the curve, all of the mixtures tended to have similar E* values. However, when moving towards the opposite range of temperatures and frequencies, slight differences can be observed, especially for the mixture containing recycled asphalt shingles. These trends can also be observed when analyzing the mastercurve regression

coefficients. Table 15 gives a summary of the mastercurve regression coefficients that were generated using the modified MEPDG mastercurve model. Goodness of fit parameters are also shown in Table 15.

Maximum E* values were similar; however, minimum E* values did show significant differences. In terms of the steepness of the curve given by the parameter -γ, the 25% RAS and 5% RAS mixture showed the lowest slope (less susceptible to changes in frequency), and the 50% RAP mixture showed the highest slope (most susceptible to changes in frequency). The inflection point frequency parameter -β/γ was the highest for the 25% RAS and 5% RAS mixture (4.55 Hz), followed by the French EME mixture (3.61 Hz); the remaining mixtures had similar inflection points around 2.85 Hz. The activation energy term is best regarded as an experimentally determined parameter that indicates the sensitivity of the shift factors to temperature, and consequently affects the shape of the mastercurve. In this case, all mixtures had similar activation energy terms, but the 25% RAP-5% RAS mixture had the highest term producing a wider range of reduced frequencies and a more flattened curve.
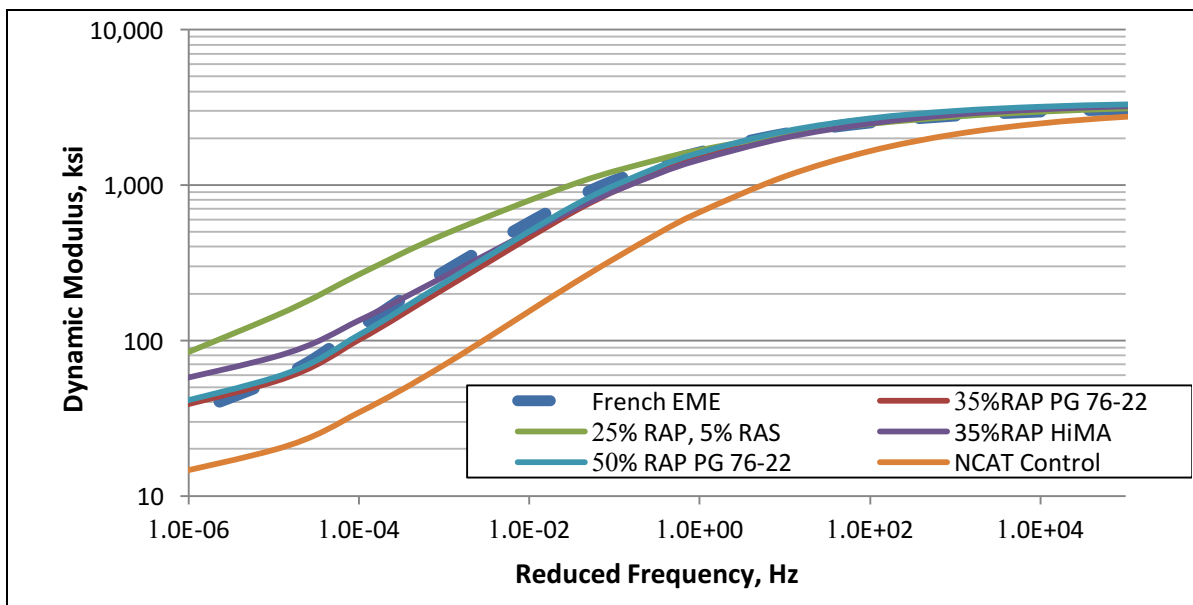
Figure 20 Dynamic Modulus Mastercurves

Table 15 Mastercurve Coefficients

Mixture ID	Max E* (Ksi)	Min E* (Ksi)	Beta	Gamma	EA	R2	Se/Sy
French EME	3240.96	8.57	-2.023	-0.560	207939.5	0.991	0.066
35%RAP PG 76-22	3417.23	17.05	-1.697	-0.595	197985.7	0.993	0.057
25% RAP, 5% RAS	3389.56	10.40	-1.972	-0.433	244676.9	0.985	0.088
35%RAP HiMA	3423.82	26.10	-1.548	-0.556	215061.3	0.997	0.041
50% RAP PG 76-22	3446.47	18.40	-1.778	-0.610	206143.0	0.993	0.058

In an attempt to identify testing variability and/or non-linearity in the material behavior due to non-compliance to the recommended micro-strain levels, the dynamic modulus and phase angle were averaged for each laboratory's data and plotted in Black Space (Airey, 2002; Christensen et al, 2003). Figure 21 contains the Black Space plots for all the different mixes including the 19.0 mm NMAS control mixture from the 2009 NCAT Test Track cycle. It should be noted that all plots show good uniformity in their respective Black Space diagrams, as noted with their R^2 values being greater than 0.94 for a 4th-order polynomial fitted function. Due to the interaction of the asphalt binder with aggregate, the Black Space diagram for a mixture shows a peak phase angle value at intermediate dynamic modulus. At high temperatures, the aggregate structure begins to dominate behavior of the mixture while at lower temperatures volumetric properties and binder stiffness control the behavior. This peak value is associated with the inflection point in the mastercurve using the terms described earlier $(-\beta/\gamma)$.French EME and 50% RAP mixtures had similar peak phase angles around 33 degrees but different peak dynamic modulus of 220 ksi and 237 ksi, respectively. For the 35% RAP mixture, this peak occurs around dynamic modulus of 230 and for the 25% RAS-5% RAS and 35% RAP HiMA mixtures, this occurs around dynamic modulus of 205 ksi and 218 ksi, respectively.

Additional analysis of the Black Space diagram indicates that mixtures with lower phase angle values are more elastic (25% RAS-5% RAS, 35% RAP HiMA mixtures). On the other hand, if the phase angle is high, the mixture is more viscous (French EME and 50% RAP mixtures) (Rahbar-Rastegar and Daniel, 2016). In addition, stiffer mixtures at lower phase angles are more susceptible to cracking (Anderson et al., 2011) In this case, the 35% RAP and 50% RAP mixtures have slightly higher moduli at low phase angles than the other mixtures.

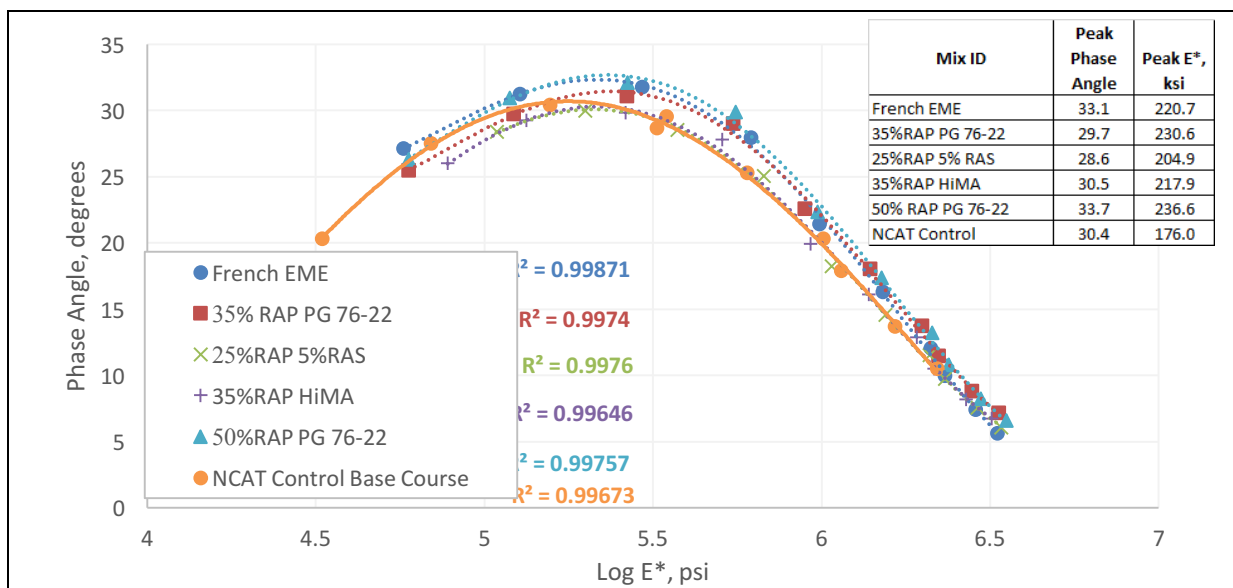| Mix ID	Peak Phase Angle	Peak E*, ksi
French EME	33.1	220.7
35%RAP PG 76-22	29.7	230.6
25%RAP 5% RAS	28.6	204.9
35%RAP HiMA	30.5	217.9
50% RAP PG 76-22	33.7	236.6
NCAT Control	30.4	176.0

Figure 21 Black Space Diagrams

To assess statistical differences, a general linear model (GLM) (α = 0.05) was conducted on the test data measured at 4°C, 20°C, and 45°C, and at two frequencies: 10 Hz and 1Hz. Thus, the GLM

was completed four times to assess statistical differences at each temperature. The Tukey-Kramer test (α = 0.05) was used to determine where these statistical differences occurred and how the mixtures grouped within each project. Table 16 shows the results of the Tukey-Kramer test on E* values for 20°C and 45°C only (results at 4°C followed similar statistical trend of results at 20°C). Mixtures given the same letter in the table were statistically grouped together (no statistical difference among mixtures at α = 0.05). As expected, at high temperatures and low frequencies, statistical differences were obtained for some of the mixtures. The results indicated that the mixture with 25% RAP and 5% RAS had the highest E* values while the mixture with 35% RAP HiMA had the lowest E* values. On the other hand, no statistical differences were obtained among mixtures at 20°C for a significance level α = 0.05.

Table 16 E* Statistical Grouping

Mixture ID	20 °C, 10 Hz		20 °C, 1 Hz		45 °C, 10 Hz		45 °C, 1 Hz	
	Mean	Group	Mean	Group	Mean	Group	Mean	Group
French EME	2,103.7	A	1,517.8	A	615.8	A B	293.1	A B
35% RAP PG 76-22	1,982.9	A	1,388.3	A	545.7	A B	264.1	B
25% RAP, 5% RAS	2,086.0	A	1,544.7	A	673.0	A	373.2	A
35% RAP HiMA	1,910.1	A	1,375.6	A	505.6	B	261.5	B
50% RAP PG 76-22	2,119.8	A	1,503.8	A	555.1	A B	265.5	B

4.4   Flow Number

The Flow number test is a rutting resistance test that is performed using the AMPT. It applies a repeated compressive loading to an asphalt specimen while the AMPT records the deformation of the specimen with each additional loading cycle. The user defines the temperature, applied stress state (deviator stress and confining stress), and number of cycles at which the test is performed. The loading is applied for a duration of 0.1 seconds followed by a 0.9 second rest period every 1 second cycle. Flow number data is commonly modeled with the Francken model, shown as Equation 11 (AASHTO TP 79-13). An example of unconfined flow number test data is shown in Figure 22.

$$\varepsilon_p(N) = aN^b + c(e^{dN} - 1)$$

(11)

where

ε_p *(N)* =   permanent strain at 'N' cycles,

N =   number of cycles, and

a, b, c, d =   regression coefficients.

The flow number is defined as the number of cycles at which the sample begins to rapidly fail and coincides with the minimum rate of strain accumulation measured during the test. This is more properly defined as the breakpoint between steady-state rutting (secondary rutting) and the more rapid failure of the specimen (tertiary flow). Figure 22 demonstrates this concept graphically. If the samples do not exhibit tertiary flow (common for confined samples), then the

amount of deformation at a specified loading cycle can still be used to give a relative ranking of tested mixtures with respect to rutting susceptibility.
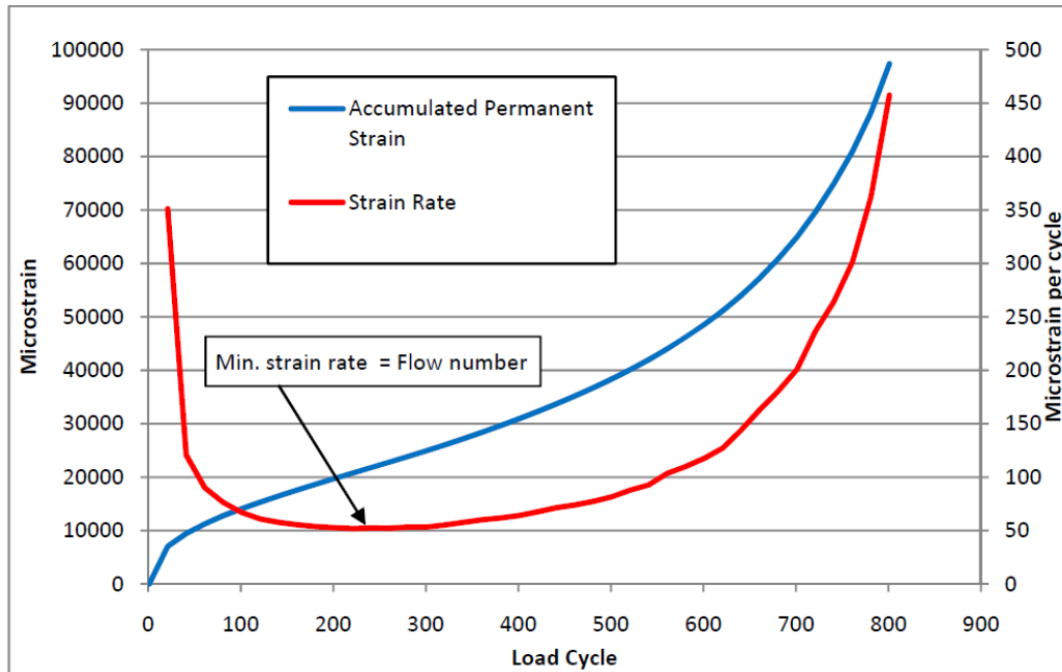
Figure 22 Typical Flow Number Test Data

Flow number testing for this project was performed in accordance with AASHTO TP 79-13 in an unconfined state with a deviator stress of 87 psi. The tests were run until either the samples reached 5% axial strain (7.5 mm of deformation on a 150 mm sample) or the test went the full 20,000 cycles. Samples were prepared in accordance with AASHTO PP 60-14 to a target air void level of 3.5 ± 0.5 percent on the final cored and trimmed specimen. By AASHTO TP 79-13, the flow number test temperature is selected based on the LTPPBind 50% reliability high pavement temperature at the project location adjusted for a 20 mm depth in the pavement structure. The Auburn, Alabama climate region was assumed to generate the flow number test temperature. The temperature data from the LTPPBind v3.1 software for Auburn is shown in Figure 22 below. Based on these criteria, the temperature of 59.5°C was selected for this project (LTPPBind temperature rounded to the nearest 0.5°C). While AASHTO TP 79-13 does contain traffic level criteria for mixtures based off their flow number results, these criteria are not completely applicable for this study since the specimens were fabricated to a different target air void content (these criteria are for specimens fabricated to 7.0 ± 0.5 percent air voids).
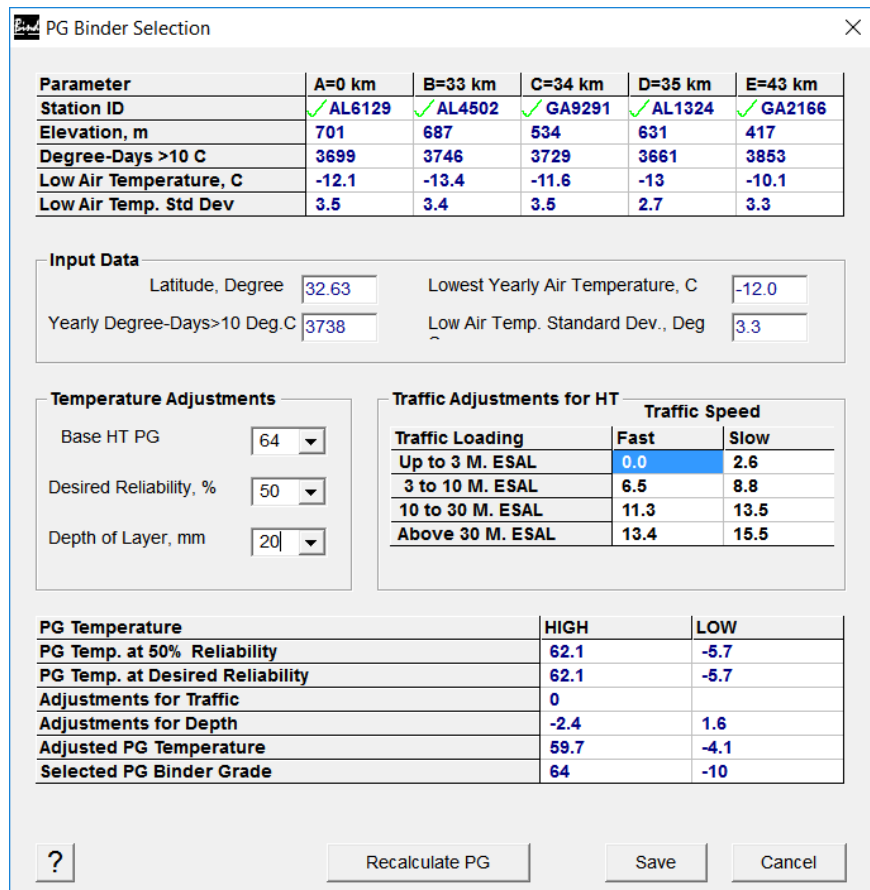
Figure 22 LTPPBind v3.1 Output for Auburn, AL Area

Table 17 shows the results of the flow number test performed on all the mixtures and the statistical grouping. The GLM (α = 0.05) showed no statistical difference between the 35% RAP and the 50% RAP mixtures. On the other hand, the remaining mixtures were statistically different from each other. The 35% RAP HiMA mixture showed the highest resistance to permanent deformation followed by the 25%-5% RAS mixture. Similar strain values were obtained for all mixtures but the French EME mixture (more ductile). All of the mixtures exhibited flow number values well in excess of the 740 recommended for a greater than 30 million ESAL design pavement by AASHTO TP 79-13. While these criteria are not completely applicable given the aforementioned air void level of the specimens, it does give some frame of reference for the high level of rutting resistance offered by these high-modulus mixtures.

Table 17 Flow Number Test Results

Mixture ID	Air Voids (%)	Francken Flow Number			Francken Microstrain at FN			FN Statistical Group
	Average	Average	Standard Deviation	CV (%)	Average	Standard Deviation	CV (%)	
French EME	3.5	4,665	716	15.3	29,381	2,271	7.7	A
35% RAP PG 76-22	3.2	1,910	577	30.2	17,648	1,365	7.7	B
25% RAP, 5% RAS	3.5	8,229	676	8.2	15,128	1,367	9.0	C
35% RAP HiMA	3.3	18,374	1,807	9.8	16,362	3,122	19.1	D
50% RAP PG 76-22	3.1	1,337	485	36.3	15,987	1,406	8.8	B

4.5 AMPT Cyclic Fatigue

Fatigue testing for this project was performed using the uniaxial tension fatigue method available in the Asphalt Mixture Performance Tester (AMPT). This method is summarized in AASHTO TP 107-14. This methodology utilizes the simplified viscoelastic continuum damage (S-VECD) model (Hou et al., 2010). Hereafter, this testing protocol will simply be referred to as AMPT cyclic fatigue S-VECD testing. AMPT cyclic fatigue analysis on a given mixture requires both dynamic modulus ($|E^*|$) testing as well as uniaxial fatigue testing. S-VECD is a mode-of-loading independent, mechanistic model that allows for the prediction of fatigue performance parameters at different temperatures and loading conditions (Jacques et al., 2016; Daniel and Kim, 2002; Underwood et al., 2012).

Specimen preparation for cyclic fatigue testing is identical to that for the AMPT specimens required for the dynamic modulus test (AASHTO PP 60-14), with the exception that the specimens are trimmed to a height of 130 mm tall instead of the standard 150 mm tall. Specimens for the high-modulus mixtures were prepared to a target air void content of 3.5 ± 0.5% after trimming. A minimum of four specimens were tested per unique mixture. Guidance in AASHTO TP 107-14 was used to select strain levels for testing that provide a range of cycles to failure (N_f).

To conduct this test, an AMPT sample is glued with a steel epoxy to two end platens. The sample and end platens are then attached with screws to the actuator and reaction frame of the AMPT prior to installing on-specimen LVDTs. A photo of this test setup is shown in Figure 23.

An AMPT sample glued with steel epoxy to rigidly mounted end platens.
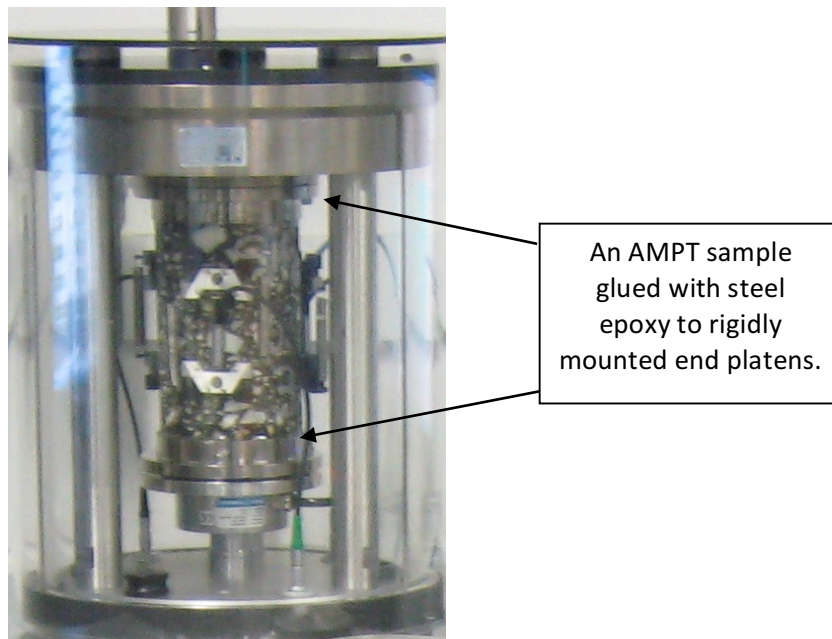
Figure 23 IPC Global® AMPT S-VECD Fatigue Test Setup

The recommended temperature for the cyclic fatigue test is the average temperature of the high and low PG grade of the base binder, minus three degrees Celsius. The maximum allowable temperature according to AASHTO TP 107-14 is 21°C. The maximum allowable temperature of 21°C was necessary in order to test the high-modulus mixtures from this study. The reason for the maximum temperature is to avoid viscoplastic effects during the test. This results in a simpler model because strain decomposition is not needed

The fatigue test is performed at a frequency of 10 Hz and consists of two phases. First, a small strain (50 to 75 on-specimen microstrain) test is performed to determine the fingerprint dynamic modulus of the sample. This is conducted to determine the ratio of the finger-print dynamic modulus ($|E^*|_{FP}$) of the testing sample to the dynamic modulus determined from AMPT dynamic modulus testing ($|E^*|_{LVE}$). This value is known as the dynamic modulus ratio (DMR) and is recommended to be between 0.9 and 1.1 (Equation 12) (Hou et al., 2010). This ratio is used for controlling the quality of the fatigue testing and is incorporated into the S-VECD fatigue model (Hou et al., 2010).

Secondly, the sample is subjected to a fatigue test in which the AMPT actuator is programmed to reach a constant peak actuator displacement with each loading cycle. During this test, the dynamic modulus and phase angle of the sample are recorded. Failure of the sample is defined as the point at which the phase angle peaks and then drops off (Hou et al., 2010). This concept is demonstrated graphically in Figure 24.

$$\mathbf{DMR} = \frac{|\mathbf{E}*|_{\mathbf{FP}}}{|\mathbf{E}*|_{\mathbf{LVE}}} \tag{12}$$
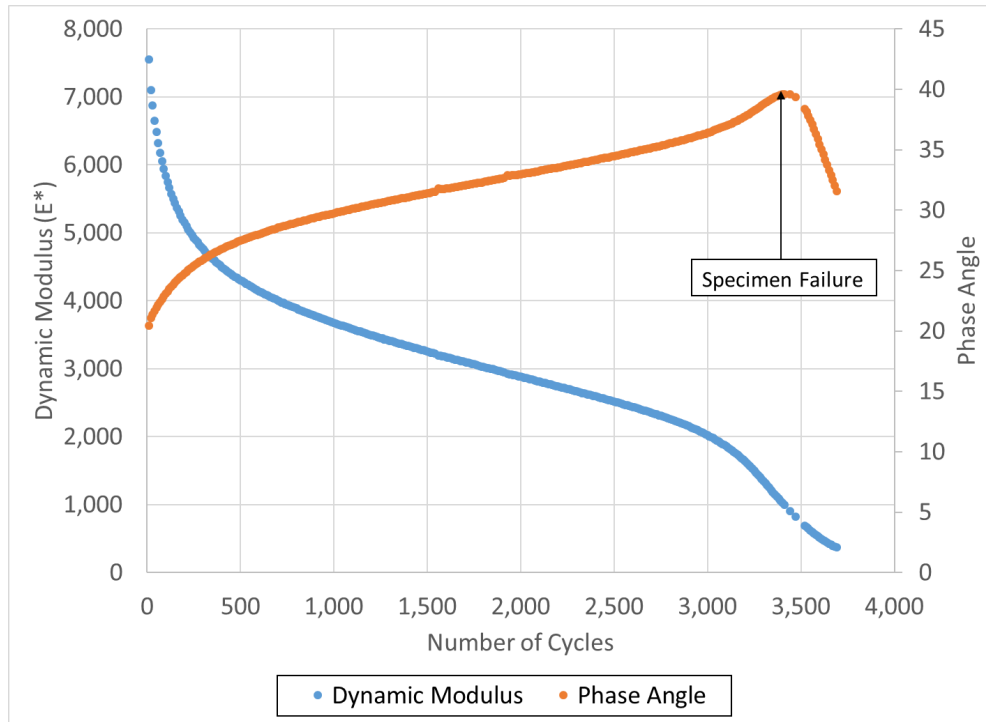
Figure 24 Determination of Cycles to Failure for S-VECD Fatigue Test

S-VECD analysis was performed using the ALPHA-Fatigue (v 3.1.5) analysis software developed by Underwood and Kim. The ALPHA-Fatigue software produces two outputs from the input dynamic modulus and fatigue tests: the damage characteristic curve and the energy-based failure criterion. The damage characteristic curve (or C vs. S curve) plots the pseudo secant modulus (C) of the mixture against its damage parameter (S). Practically, this illustrates how fatigue damage evolves in a unique asphalt mixture (Jacques et al., 2016). For this study, this model was generated using an exponential function (Equation 13).

$$C = e^{aS^b}$$ (13)

where

C = pseudo secant modulus,
S = damage parameter, and
a, b = model coefficients.

The second output from the ALPHA-Fatigue software is energy-based failure criterion, or G^R method (Sabouri and Kim, 2014). The G^R term is defined as the rate of change of the averaged released pseudostrain energy (per cycle) throughout the test (Sabouri and Kim, 2014). The G^R term characterizes the overall rate of damage accumulation through fatigue testing (Jacques et al., 2016). A plot of G^R versus cycles to failure (N_f) can be generated from the ALPHA-Fatigue analysis, and the slope and position of these curves can be used to gage the relative fatigue resistance of one mixture to another (Jacques et al., 2016).

A summary of the results from the individual S-VECD tests is included in Table 18 below. Of the 24 individual specimens tested, 16 specimens had a DMR value in the recommended range (0.9 to 1.1). The remaining eight specimens had borderline DMR values of between 0.84 and 0.90, indicating a maximum 16% disconnect between the mixture E* tested during dynamic modulus and E* verified during the fatigue testing. These results were not excluded for two reasons. First, the testing was being performed on unique (high-modulus) materials at a non-standard air void content. Secondly, these specimens were not detrimental to the quality of the G^R versus N_f model discussed hereafter.

The damage characteristic (C vs. S) curves for this project are shown in Figure 25 while the energy release (G^R vs. N_f) curves are shown in Figure 26. A power model of standard form was fit to the G^R versus N_f curves, with the model coefficients summarized in Table 19. Figure 25 shows three of the mixtures (35% RAP PG 76-22, 50% RAP PG 76-22, and 25% RAP-5% RAS PG 76-22) to have virtually identical damage characteristic curves, while the EME 14 and 35% RAP HiMA mixtures have the greatest stiffness as additional damage is applied to the specimens. The energy release curves all had power model R^2 values of 0.94 or above, indicating a good model fit. The curve with the highest slope and highest intercept was the EME 14 mixture. This indicates that at low energy release rates (10 or 100), this mixture has poor fatigue resistance relative to the other mixture designs. Three of the mixtures (50% RAP PG 76-22, 25% RAP-5% RAS PG 76-22, and 35% RAP HiMA) had virtually identical slopes at the low end of the spectrum, indicating improved fatigue resistance relative to the other two mixtures. The 35% RAP HiMA mixture had the highest intercept of this grouping of three mixtures and is further to the right of the plot in Figure 26, indicating it would be the most fatigue resistant mixture in this grouping.

Table 18 Summary of S-VECD Individual Test Results

| Mixture ID	Specimen ID	Air Voids (%)	$|E^*|_{LVE}$ (MPa)	$|E^*|_{FP}$ (MPa)	DMR	N_f	G^R
EME 14	9	3.0	14,694	14,715	1.001	7,795	270.9
EME 14	11	3.8	14,643	14,102	0.963	47,682	12.9
EME 14	12	3.9	14,694	14,172	0.964	2,835	489.7
EME 14	13	3.7	14,694	14,614	0.995	73,284	6.8
35% RAP PG 76-22	326	3.2	13,954	11,904	0.853	47,685	20.0
35% RAP PG 76-22	327	4.0	13,954	13,314	0.954	1,175	2,037.9
35% RAP PG 76-22	328	4.0	13,954	11,952	0.857	11,500	217.0
35% RAP PG 76-22	329	4.0	13,899	11,992	0.863	39,060	33.1
35% RAP PG 76-22	330	4.0	13,954	11,795	0.845	6,035	282.6
50% RAP PG 76-22	221	3.5	14,939	14,374	0.962	3,275	654.0
50% RAP PG 76-22	222	3.2	14,939	15,161	1.015	3,795	333.3
50% RAP PG 76-22	223	3.3	14,882	12,484	0.839	214,224	4.7
50% RAP PG 76-22	224	3.7	14,882	13,001	0.874	40,900	34.6
50% RAP PG 76-22	225	3.2	14,939	14,021	0.939	69,991	36.4
25% RAP-5% RAS PG 76-22	128	3.1	14,815	13,458	0.908	795	2,644.8
25% RAP-5% RAS PG 76-22	131	3.8	14,815	12,501	0.844	1,195	747.2
25% RAP-5% RAS PG 76-22	132	3.9	14,764	12,532	0.849	4,195	317.5
25% RAP-5% RAS PG 76-22	134	3.9	14,764	13,282	0.900	78,330	14.0
25% RAP-5% RAS PG 76-22	135	3.4	14,764	13,233	0.896	4,075	610.7
25% RAP-5% RAS PG 76-22	136	3.8	14,764	13,303	0.901	1,655	1,385.5
35% RAP HiMA	421	3.6	13,454	12,869	0.957	55,031	33.5
35% RAP HiMA	422	3.2	13,563	13,014	0.960	1,635	1,730.3
35% RAP HiMA	423	3.4	13,454	13,788	1.025	7,295	521.0
35% RAP HiMA	425	3.5	13,398	12,694	0.947	3,255	462.4
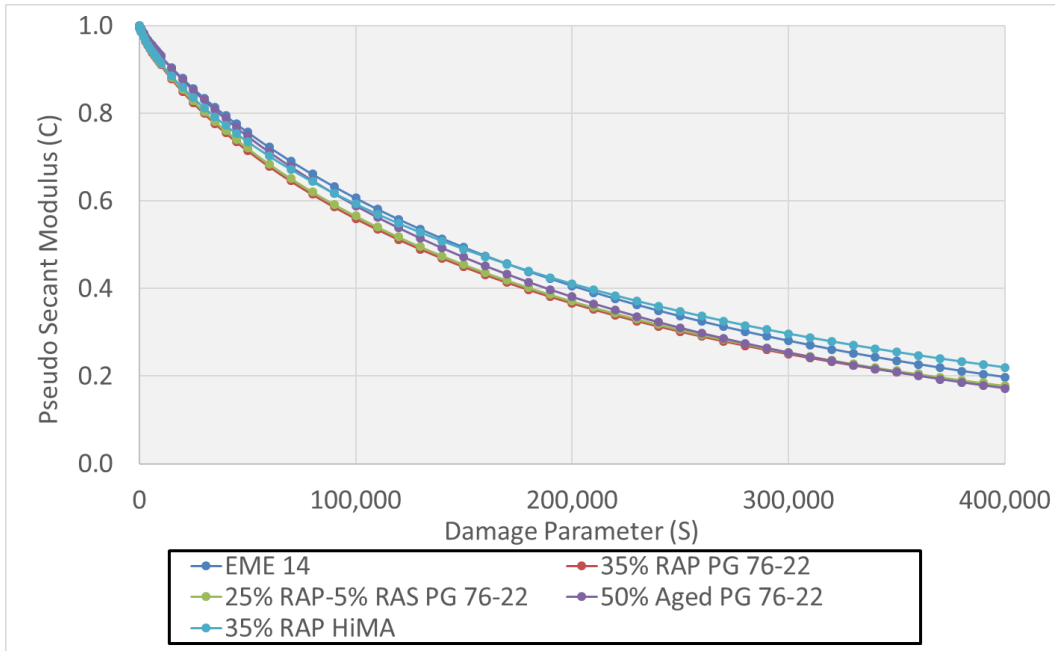
Figure 25 S-VECD: C versus S Curves
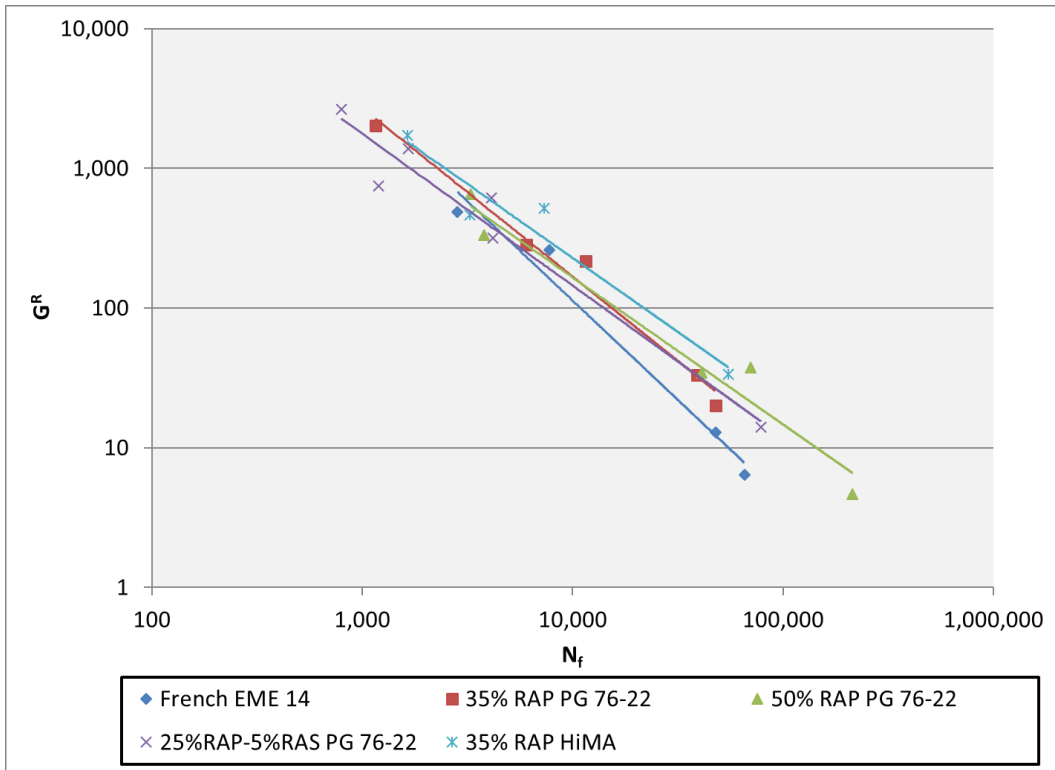
Figure 26 S-VECD: G^R versus N_f Curves

Table 19 Summary of S-VECD G^R vs. N_f Power Model Coefficients

Mixture ID	α_1	α_2	R^2
French EME	-1.422	5.512E+07	0.973
35% RAP PG 76-22	-1.207	1.135E+07	0.981
50% RAP PG 76-22	-1.053	2.695E+06	0.963
25% RAP-5% RAS PG 76-22	-1.087	3.229E+06	0.951
35% RAP HiMA	-1.059	3.925E+06	0.940

5.   AASHTOWARE PAVEMENT ME DESIGN ANALYSIS

One of the objectives of this study was to use the AASHTOWare Pavement ME Design software to determine how a high-modulus base can affect the performance of asphalt pavements. To achieve this objective, the Pavement ME Design file for section S9 in the 2009 NCAT Test Track was utilized to perform the simulation. Level 1 input was used in the Pavement ME simulations for all layers. The measured dynamic modulus in Section 4.3 was used in the simulation of high-modulus base layers in Pavement ME Design software. Five years of design life were used in the simulation. Pavement construction information is shown in Table 20.

Six simulated scenarios were used to determine the effect of different high-modulus base mixtures on the performance of asphalt pavements. Each scenario is explained as follows:

1. Simulation 1 utilized material properties from the 2009 Test Track Cycle Section S9 (control section).
2. Simulation 2 was designed to determine how a high-modulus mixture designed based on a French mixture design procedure can affect the performance predicted by Pavement ME Design.
3. Simulation 3 was designed to determine how a 35% RAP mixture can affect the performance predicted by Pavement ME Design. The binder grade was PG 76-22 and the mixture was labeled 35% RAP PG 76-22 No Lime.
4. Simulation 4 was planned to determine how a 25% RAP + 5% RAS mixture can affect the performance predicted by Pavement ME Design. The binder grade was also PG 76-22 and the mixture was labeled 50% Aged Binder PG 76-22 No Lime.
5. Simulation 5 was planned to determine how a 35% RAP with high polymer-modified asphalt binder (HiMA) mixture can affect the performance predicted by Pavement ME Design. The mixture utilized SBS from Kraton with No Lime.
6. Simulation 6 was designed to determine how a 50% RAP mixture can affect the performance predicted by Pavement ME Design. The binder grade was PG 76-22 and the mixture was labeled 50% RAP PG 76-22 No Lime.

Table 20 Simulation Plan

	Simulation 1	Simulation 2	Simulation 3	Simulation 4	Simulation 5	Simulation 6
Name	Control base	French EME	35% RAP	25% RAP, 5% RAS	35% RAP HiMA	50% RAP
Surface AC: 1.2 in	9.5 mm PG 76-22					
Binder AC: 2.8 in	19 mm PG 76-22					
Base AC: 3.0 in	Unmodified Mixture PG 67-22	French EME 14	35% RAP PG 76-22 No Lime	50% Aged Binder PG 76-22 No Lime	35% RAP Kraton No Lime	50% RAP PG 76-22 No Lime
Base Binder PG	PG 67-22	PG 88-16	PG 76-22	PG 76-22	PG 94-28	PG 76-22
Granular base: 5.8 in	Crushed stone granular base					
Subgrade	Test Track subgrade					

5.1 Traffic

The truck fleet at the NCAT Test Track runs at a target speed of 45 mph, and operates 16 hours daily, six days a week for each two-year cycle. Each of the trucks completes about 680 miles per day so as to apply 10 million ESALs collectively in two years. Thanks to simple truck patterns and running schedules, input Level 1 for traffic information was precisely characterized for the MEPDG analysis. Traffic information is displayed in Table 21. Trafficking at the 2009 NCAT Test Track was conducted using four triple flat-bed trailer trucks (Figure 27) and one triple box trailer loaded the pavement from Monday to Saturday. Table 22 provides the axle weights for each of the five trucks under normal loading conditions.

Figure 27 Triple Flat-Bed Trailer Truck at NCAT Test Track

Table 21 Traffic Information

Age (year)	Heavy Trucks (cumulative)
2009 (initial)	3,082
2011 (2 years)	2,814,250
2014 (5 years)	5,628,500

Table 22 Axle Weights (lbs) for Trucking Fleet at NCAT Test Track

Truck #	Steer	Front Drive Tandem	Rear Drive Tandem	Single # 1	Single # 2	Single # 3	Single # 4	Single # 5
1	9,400	20,850	20,200	20,500	20,850	20,950	21,000	20,200
2	11,200	20,100	19,700	20,650	20,800	20,650	20,750	21,250
3	11,300	20,500	19,900	20,500	20,500	21,000	20,650	21,100
4	11,550	21,200	19,300	21,000	21,050	21,000	20,750	20,800
5	11,450	20,900	19,400	20,100	20,450	21,000	20,050	20,650
Average	11,450	20,900	19,400	20,100	20,450	21,000	20,050	20,650

In order to represent a triple trailer, two fictitious vehicle classes were used together with five single axles and one tandem axle from the Class 13, and the remaining one single axle from the Class 12. The average axle width was 8.5 ft, the dual tire spacing was 13.5 in, and the tire pressure was approximately 100 psi. Other traffic inputs (i.e., lateral traffic wander) were assumed to be routine design values, and they were left as the defaults provided by the MEPDG. There was no annual traffic growth.

5.2   Climate

The climatic data required in the MEPDG is used by the Enhanced Integrated Climate Model (EICM) to calculate changes in the temperature and moisture profile throughout the pavement cross section. The climatic input for the MEPDG is actually a file that contains a recorded history of temperature, rainfall, wind speed, humidity, and sunlight conditions for a specific area. There are two ways to prepare the climatic inputs for the MEPDG, either by selecting a climatic data file for representative areas or by preparing a new climatic data file based on a local weather station. The latter was adopted in this study because the Test Track has an on-site weather station (Figure 28), which is responsible for collecting environmental information on an hourly basis. The Test Track is at a geographic coordinate of 32°59´N, -85°30´W, and an elevation of 600 ft. The next section will cover the method to prepare a climate file for a particular condition.

Figure 28 Test Track On-Site Weather Station

It is noted that two formats of files function in the MEPDG: the ICM file and the hourly climatic database file. The ICM file was generated by the MEPDG calculation based on an hourly climatic database file. In fact, the hourly climatic database file was either given for those representative areas or can be self-developed.

AASHTOWare Pavement ME Design software was used to compute the following distresses to simulate the pavement performance over a five-year period of analysis:

- International Roughness Index (IRI),
- Top-down cracking,
- Bottom-up fatigue cracking,
- Thermal cracking,
- Total pavement rutting, and
- Rutting in the asphalt concrete layer.

5.3   Estimated Performance

Figure 29 shows the estimated layer moduli for all six scenarios. As expected, all of the high-modulus base courses exhibit higher layer moduli throughout the five-year performance period of analysis. The results indicate that high-modulus base courses can have higher layer moduli ranging from 1.5 to 2.0 times the layer modulus of the control section. However, no significant differences among the high-modulus mixtures can be observed. Further analysis indicates that the 35% RAP HiMA mixture exhibits lower layer moduli, especially at high temperatures, compared to the remaining high-modulus mixtures. This behavior is in agreement with the dynamic modulus test results for the high temperature low frequency range. However, the 25% RAP-5% RAS base course does not exhibit higher modulus at the low temperature high frequency as expected from the E* test results.
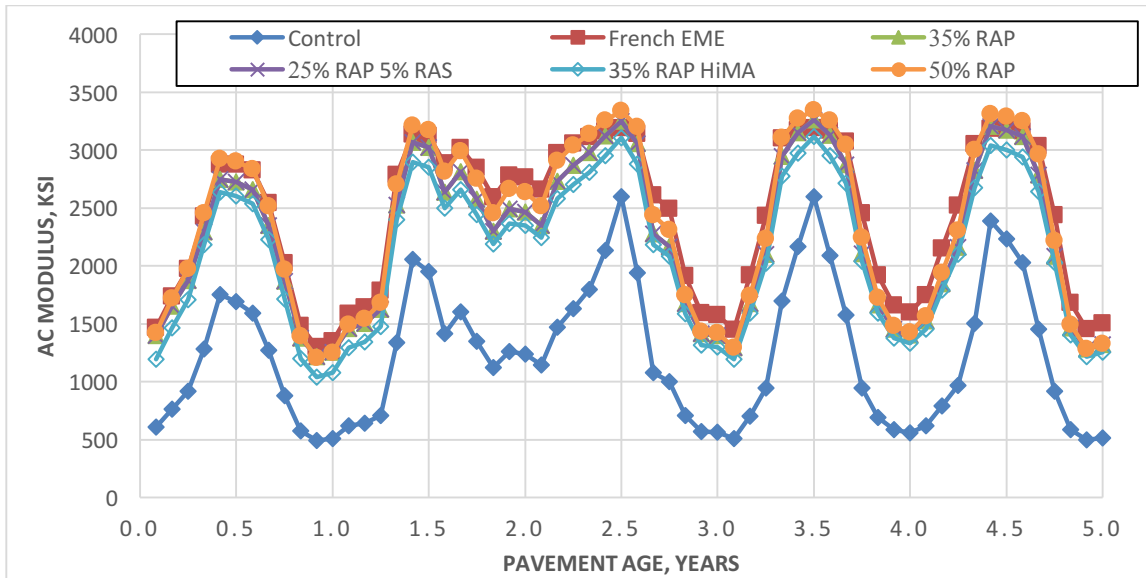
Figure 29 Estimated Base AC Layer Modulus

Cracking of the asphalt layer was expected to decrease by the use of high-modulus base courses. Figures 30 and 31 show estimated results of cracking. It was observed that the use of high-modulus base courses could reduce the bottom-up cracking, which was reasonable since high-modulus base may reduce the tensile stress and strain at the bottom of the binder layer. This reduction in cracking could range from 20% to 25%. Moreover, it can be observed that the effect on top-down cracking can be more significant with a decrease in cracking ranging from 28% to 35%. In this case, the 35% RAP HiMA mixture seems to be the least resistant to fatigue cracking of all HMAC mixtures and the EME mixture seems to show the best performance, contrary to the results obtained with the S-VECD test results. However, the observed trends in fatigue cracking performance for the five high-modulus designs can be considered similar for practical purposes.
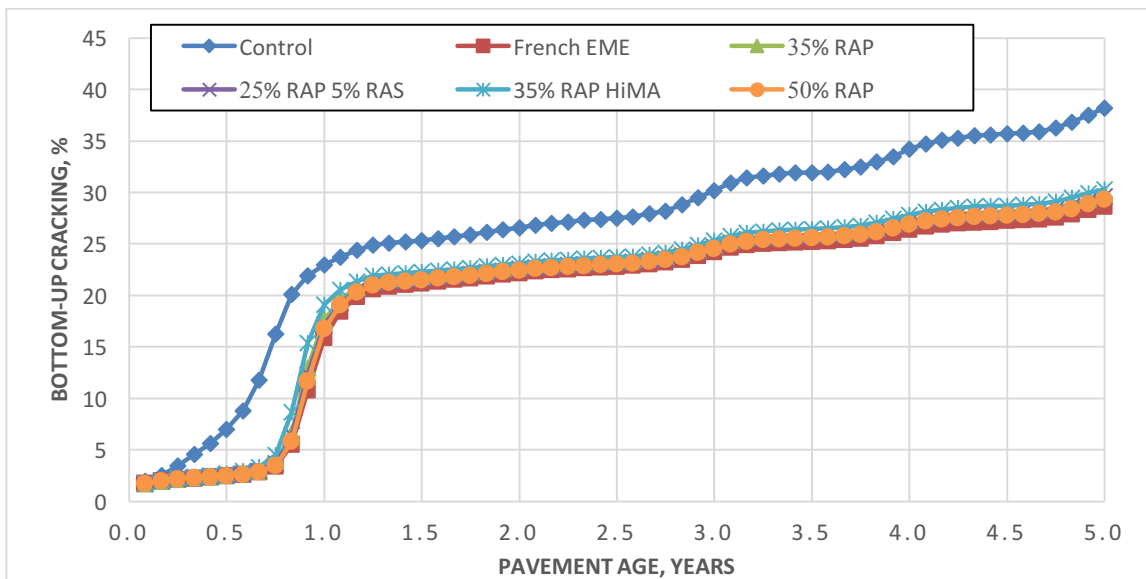

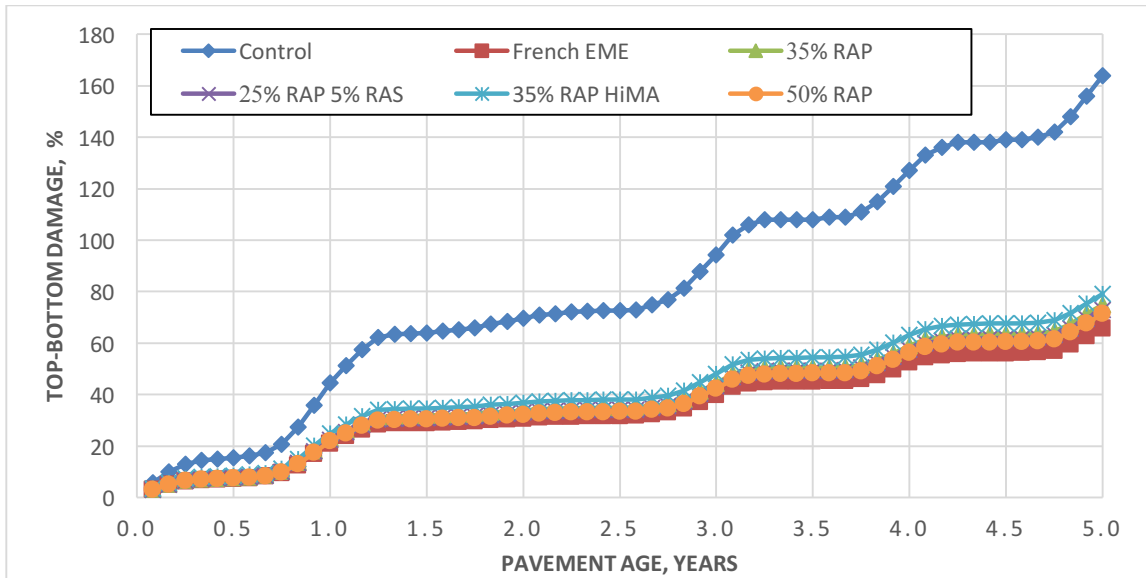**Figure 30 Estimated Bottom-Up Fatigue Cracking**

51

Figure 31 Estimated Top-Down Fatigue Damage

Figure 32 shows the estimated results of permanent deformation of the asphalt concrete layer. It was observed that using high-modulus base layer materials would have no significant effect on the rutting of the entire asphalt concrete section. This can be explained by the small observed differences among high-modulus base courses as well as the use of the same top and intermediate AC layers in the simulations. A reduction in less than 4% of the AC layer rut depth was estimated. When comparing the simulated permanent deformation and the results from the flow number testing, no correlation in the results was evident.
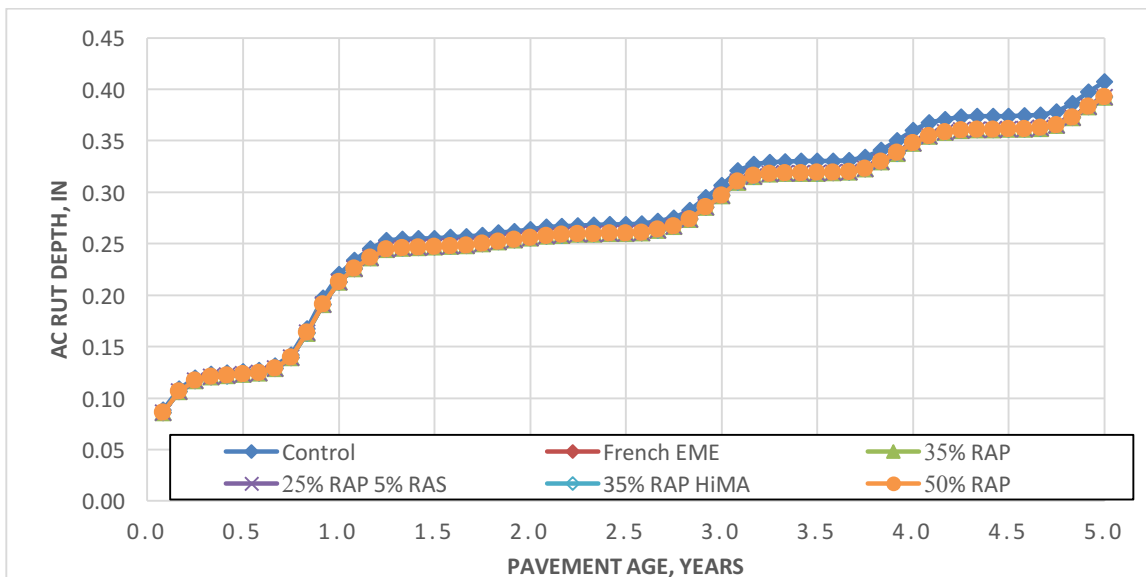

Figure 32 Estimated Permanent Deformation of the Entire AC Layer

Figure 33 shows the predicted performance of the six pavement structures in terms of IRI. It was observed that the use of a high-modulus base can reduce the IRI from 5.6% to 6.7% relative to

the control section, and no significant difference in IRI was found in the simulations among high-modulus base courses.
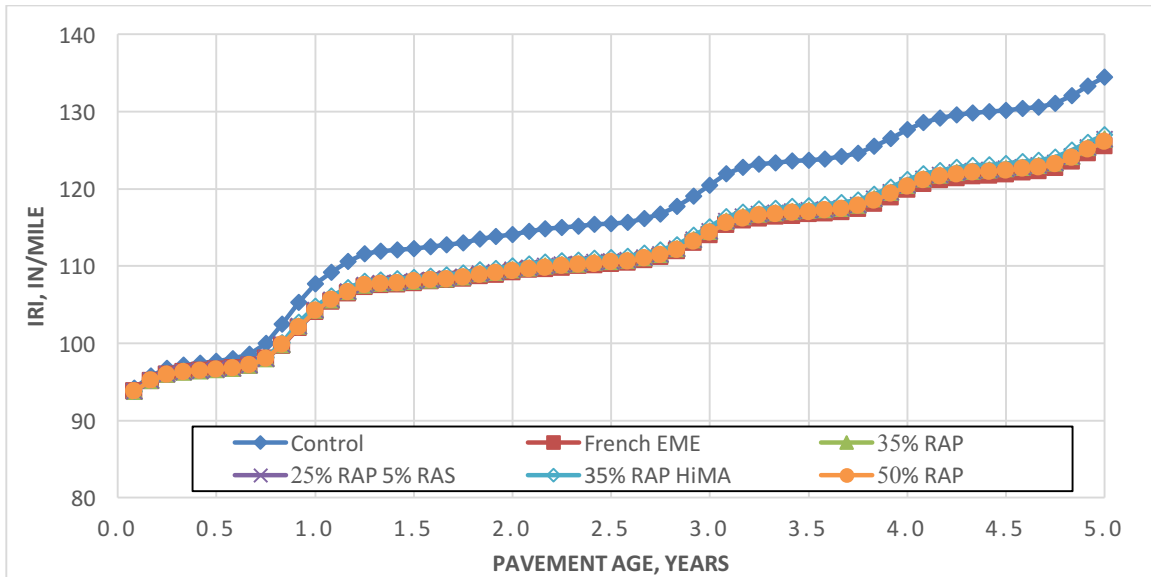
**Figure 33 Estimated Surface Roughness**

Finally, Table 23 contains a summary of thermal cracking performance and percent change with respect to the control section. As shown in this table, high-modulus base courses may have no effect on the thermal cracking. This is expected since all the simulations had the same surface and binder layers whose properties mainly affect the development of thermal cracking.

Table 23 Summary of Estimated Performance

Distress Type	Target	Predicted					
		Control	French EME	35% RAP	25% RAP 5% RAS	35% RAP HiMA	50% RAP
Terminal IRI (in/mile)	172	134.49	125.51	126.56	126.37	127.02	126.13
Permanent deformation: total pavement (in)	0.75	0.57	0.55	0.55	0.55	0.55	0.55
AC bottom-up fatigue cracking (% lane area)	25	38.21	28.61	29.81	29.61	30.31	29.31
AC thermal cracking (ft/mile)	0	27.17	27.17	27.17	27.17	27.17	27.17
AC top-down fatigue cracking (ft/mile)	2000	10304	6695	7202	7099	7419	7006
Permanent deformation: AC only (in)	0.25	0.46	0.44	0.44	0.44	0.44	0.44
		Percent Reduction vs. Control					
Terminal IRI (in/mile)			6.7%	5.9%	6.0%	5.6%	6.2%
Permanent deformation: total pavement (in)			3.5%	3.5%	3.5%	3.5%	3.5%
AC bottom-up fatigue cracking (% lane area)			25.1%	22.0%	22.5%	20.7%	23.3%
AC thermal cracking (ft/mile)			0.0%	0.0%	0.0%	0.0%	0.0%
AC top-down fatigue cracking (ft/mile)			35.0%	30.1%	31.1%	28.0%	32.0%
Permanent deformation: AC only (in)			3.6%	3.6%	3.6%	3.6%	3.6%

Figure 34 measured distresses on section S9 at the NCAT Test Track from 2009 to 2014. It can be observed that performance was highly overestimated for section S9. The maximum measured rut depth was 0.34 inches of the entire structure, while the estimated maximum rut depth was 0.56 inches. Measured IRI started at 60 in/mile and did not change significantly over time with a final IRI of 80 in/mile. On the contrary, the initial estimated IRI was 94 in/mile, which was expected to increase over time to reach a final IRI of 135 in/mile. Finally, it can be observed that cracking showed the largest offset. Initial measured cracking was observed after 11 million ESALs or more than two years of truck trafficking and reaching only 10%, while cracking is expected to appear during the first year and significantly increase over time. These results can be explained due to the application of nationally calibrated transfer functions or default functions in the employed software. Therefore, not only is local calibration required for section S9, but calibration of the HMAC mixtures used in this study may be needed to further reflect their benefit as base courses.

a.

b.

c.
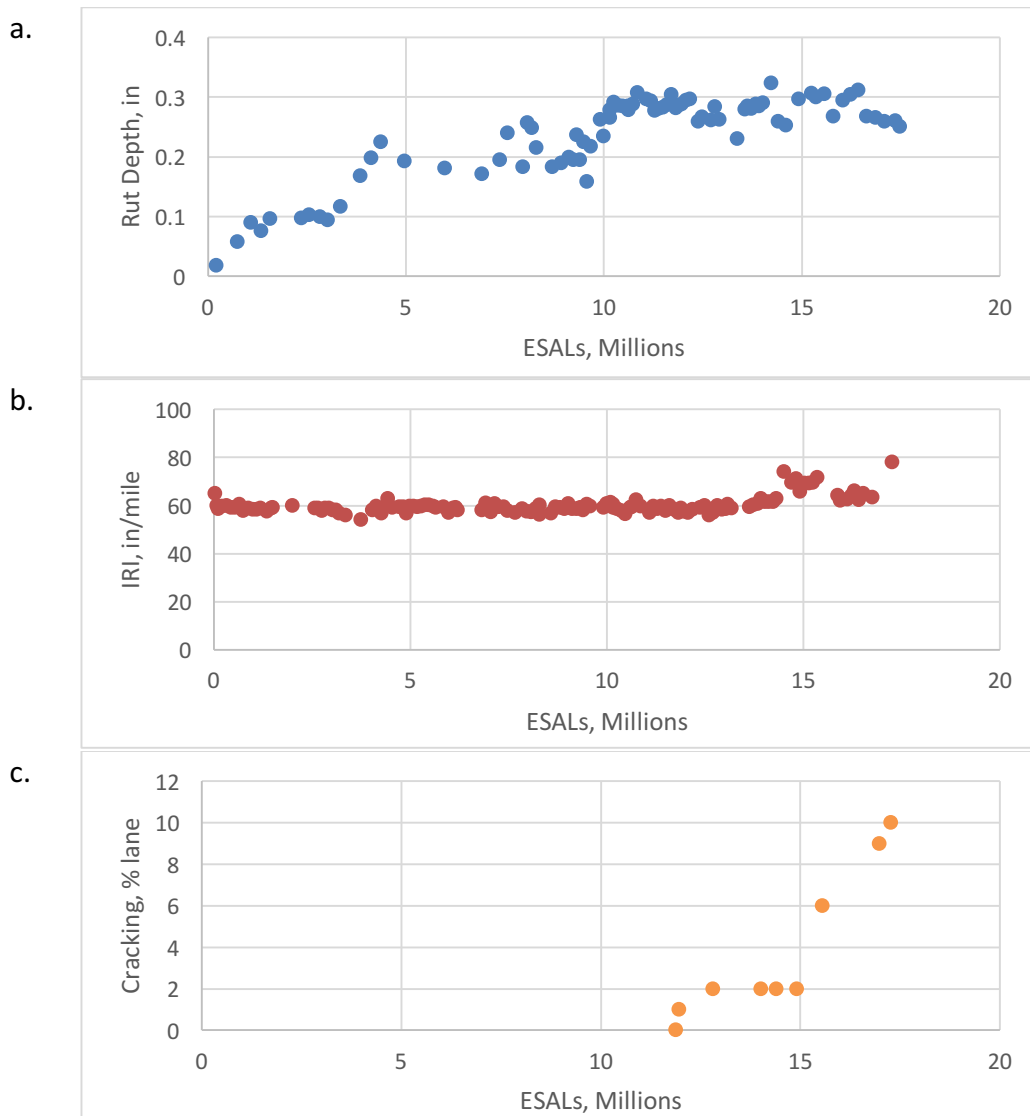
Figure 34 Measured Pavement Performance on Section S9: a. Rutting, b. Roughness, c. Cracking

In summary, the use of high-modulus base courses could improve the overall performance of an asphalt concrete layer and the entire flexible pavement structure. The type of distress that may be the most affected is top-bottom cracking followed by bottom-up fatigue cracking. Ride quality can also be slightly improved (lower IRI), and no significant effect on rutting and thermal cracking should be expected.

In Pavement ME, the performance prediction uses transfer functions that are calibrated with the existing performance data in which stiffer layers correspond to better pavements. Figure 29 showed lower modulus for the 35% RAP HiMA mixture, and as calibrated, Pavement ME predicted least resistant to fatigue cracking (higher cracking). However, the uniaxial fatigue test showed that the 35% RAP HiMA mixture is the most fatigue resistant, even though the layer moduli is lower.

With the empirical nature of the Pavement ME transfer functions, performance of new materials cannot be reliably modelled with the current transfer functions. A high modulus brittle material will have different fatigue behavior than a high modulus ductile material. Therefore, the current transfer functions in Pavement ME should be calibrated with laboratory and field performance of HMAC mixtures to have reliable predictions. The better Pavement ME predicted performance of the new material is likely a combination of its higher modulus and also an artifact of not so applicable transfer function. Until the latter is resolved, quantifying the field performance of the former through Pavement ME would be somewhat inconclusive.

6. CONCLUSIONS AND RECOMMENDATIONS

The objective of this project was to develop and validate mixture designs and evaluate predicted performance effects of high-modulus base layers. Based on experimental results and structural analysis, the following conclusions and recommendations are made:

- European mix design standard methods and specifications were successfully implemented on local (U.S.) materials. The Level 3 requirement for dynamic modulus, 14,000 MPa at 15°C and 10 Hz, was met for all HMAC mixtures.
- Reclaimed asphalt pavement can be used to stiffen the asphalt binder sufficiently for high-modulus asphalt mixtures. The minimum RAP content utilized in this investigation was 35%.
- No significant differences in dynamic modulus were obtained for all HMAC mixtures at low temperature and high frequency. However, on the opposite side of the temperature/frequency spectrum, the 25% RAP, 5% RAS mixture provided significantly higher E* values due to the inclusion of RAS.
- Flow number test results were significantly greater than those of the conventional mixture.
- Based on AMPT cyclic test results, fatigue properties among HMAC mixtures seemed to improve for the high polymer-modified mixtures and seemed to decrease for the EME French mixture, which has a stiffer virgin binder.
- Increased stiffness of HMAC mixtures improves MEPDG predicted performance of pavement in rutting, fatigue cracking, and ride quality compared to conventional base courses. A great improvement in fatigue cracking (top down and bottom up) and some improvement in rutting and ride quality.
- Correlations between laboratory performance trends among HMAC mixtures and predicted structural performance were not obtained. This was attributed to the significant role that other materials/properties have on pavement responses and performance. For instance, lower modulus for 35% RAP HiMA mixture and as calibrated Pavement ME predicted higher cracking. However, the uniaxial fatigue test showed that the 35% RAP HiMA mixture is the most fatigue resistance even though the layer moduli is lower.
- Calibration of MEPDG transfer functions applicable to HMAC mixtures is recommended to obtain more representative performance predictions.

- Based on the results of this study, a detail cost and benefit assessment is recommended in order to further quantify the effect the HMAC mixtures have on potential long-lasting perpetual-type flexible pavements.
- This study was based on a laboratory experiment. The ability to produce HMAC mixtures through a hot mix plant and to successfully lay and compact them in the U.S. has not been demonstrated. Mixing and compacting in the laboratory suggest that field operations would be more difficult with HMAC mixtures; the EME's design and testing has to be adapted to U.S. standards and conditions.

7.   RECOMMENDED MIXTURE DESIGN PROCEDURE

Based on the results of this research study and the current state-of-the-practice, the following steps are recommended as HMAC mixture design procedure:

1. Determine the aggregate trial blend for the HMAC mixture.
2. Determine the minimum asphalt binder content using the French method based on the aggregate surface area (Equations 1 to 4). However, the Asphalt Institute Hveem-Edward equation can be used successfully here.
3. Set N_{des} with the Superpave gyratory compactor to 80 gyrations and compact design samples to target air voids lower than 6%.
4. Prepare three trial dynamic modulus samples compacted to 3.0 - 6.0% air voids according to the French methodology and test at 15°C and 10 Hz.
5. Select optimum binder content to meet E* = 14,000 MPa (at 15°C and 10 Hz) to meet the minimum asphalt content from step 2 and to meet N_{des} specimens target air voids lower than 6%.
   a. Adjusting the gradation or mixture components (additives, recycled material, binder grade, etc.) may be necessary to meet E* and air voids requirements.
   b. For each gradation adjustment, the minimum AC required will need to be recalculated.
6. Select laboratory performance tests and criteria (rutting, cracking, and moisture damage) for further verification and conduct AASHTO TP 79-15 to determine dynamic modulus to be used in ME simulations.

ME simulations should be used for relative comparison purposes and not for structural pavement design until field validation has been performed. Pilot projects are a proven tool for validating and fine-tuning new practices resulting from research. Using traditional projects as a benchmark, pilot projects or programs have been used extensively to measure the relative success of new specifications and test methods. The results of pilot projects have served to effectively promote the long-term implementation of new industry practices. It is recommended that an agency champion the use of the proposed standard methodologies for design, analysis, construction, and specifications related to HMAC impact on pavement performance.

REFERENCES

Airey, G. D. Use of Black Space Diagrams to Identify Inconsistencies in Rheological Data. *Road Materials and Pavement Design*, Vol. 3, No. 4, 2002, pp. 403-424.

Anderson, R. M., G. N. King, D. I. Hanson, and P. B. Blankenship. Evaluation of the Relationship between Asphalt Binder Properties and Non-Load Related Cracking. *Journal of the Association of Asphalt Paving Technologists*, Vol. 80, 2011, pp. 615-664.

Bankowski, W., M. Tusar, L. G. Wiman, D. Sybilski, M. Gajewski, R. Horodecka, M. Maliszewksi, and K. Mirski. *Laboratory and Field Implementation of High Modulus Asphalt Concrete. Requirements for HMAC Mix Design and Pavement Design*. European Commission Research, Paris, 2009.

Brosseaud, Y. Small Overview of High Modulus Asphalt Mixes EME. Presented at Australian Scan Tour, June 2012.

Brosseaud, Y., F. Farcas, and V. Mouillet. High Modulus Asphalt Mixes with High Rate of RA: What Does it Happen? In *Congrès Eurobitume Eurasphalt*, EE2012, Turkey, October 2012.

Bueche, N., A. G. Dumont, A. Vanelstraete, J. de Visscher, S. Vansteenkiste, F. Vervaecke, J. Maek, L. Gaspar, and F. Thogersen. Laboratory and ALT-Evaluation of High Stiffness Underlayers with High Percentage of Re-use as Developed in the NR2C-Project. *Proceedings of the 4th Eurasphalt and Eurobitume Congress*, Copenhagen, Denmark, 2008.

Capitãio, S. D., and L. Picado-Santos. Assessing Permanent Deformation Resistance of High Modulus Asphalt Mixtures. *Journal of Transportation Engineering*, Vol. 132, No. 5, 2006, pp. 394-401.

Carbonneau, X., J. P. Michaut, T. Anderson, C. Thorup, and L. Ladenhoff. High Modulus GAB II: A Danish Experiment. *Proceedings of the 4th Eurasphalt and Eurobitume Congress*, Copenhagen, Denmark, 2008.

Chappat, M., X. Carbonneau, and Y. Lefuevre. Analysis of the Measured Performance of High Modulus Asphalt (HMA) and Road Base Asphalt (RBA) and a Proposal for a Compensation Principle. *European Roads Review*, 14, 2009, pp. 72-83.

Christensen Jr., D. W., T. Pellinen, and R. F. Bonaquist. Hirsch Model for Estimating the Modulus of Asphalt Concrete. *Journal of the Association of Asphalt Paving Technologists*, Vol. 72, 2003, pp. 97 – 121.

Corté, J. Development and uses of Hard-Grade Asphalt and of High-Modulus Asphalt Mixes in France. *Transportation Research Circular*, 503, 2001, pp. 12-31.

Daniel, J. S., and Y. R. Kim. Development of a Simplified Fatigue Test and Analysis Procedure using a Viscoelastic Continuum Damage Model. *Journal of the Association of Asphalt Paving Technologists*, Vol. 71, 2002, pp. 619–650.

DeBacker, C., L. Glorie, and R. Reynaert. Test sections in High-Modulus Asphalt: A Comparative Experiment with Ten Variants. *Proceedings of the 4th Eurasphalt and Eurobitume Congress*, Copenhagen, Denmark, 2008.

DeBacker, C., J. De Visscher, L Glorie, A. Vanelstraete, S. Vansteenkiste, and L. Heleven. A Comparative High-Modulus Asphalt Experiment in Belgium. In *Proceedings of Transport Research Arena Europe*, 2008, pp. 21-24.

De La Roche, C., H. Odeon, J. Simoncellli, and A. Spernol. Study of the Fatigue of Asphalt Mixes Using the Circular Test Track of the Laboratoire Central des Ponts et Chaussées in Nantes, France. *Transportation Research Record 1436*, TRB, National Research Council, Washington D.C., 1994, pp. 17-27.

De Visscher, J., S. Vansteenkiste, and A. Vanelstraete. Test Sections in High-Modulus Asphalt: Mix Design and Laboratory Performance Tests. *Proceedings of the 4th Eurasphalt and Eurobitume Congress*, Copenhagen, Denmark, 2008.

Delorme, J. L., C. De La Roche, and L. Wendling. *LPC Bituminous Mixtures Design Guide*. Laboratoire Central des Ponts et Chaussées, Paris, 2007.

Denneman, E., M. Nkgapele, J. Anochie-Boateng, and J. W. Maina. Transfer of High Modulus Asphalt Mix Technology to South Africa. In *Proceedings of the 10th Conference on Asphalt Pavements for Southern Africa*, Champagne Sports Resort, Central Drakensberg, South Africa, 2011.

Denneman, E. High Modulus Asphalt (HiMA) Trial: Mix and Pavement Design. Presented at the 22nd Meeting of the Roads Pavements Forum (RPF), Pretoria, November 2011.

Denneman, E., and M. Nkgapele. *Interim Guide for the Design of High Modulus Asphalt Mixes and Pavements in South Africa.* Report CSIR/BE/IE/ER/2010/0042/B, 2011.

Des Criox, P., and L. Planque. Experience with Optimized Hard Grade Bitumens in High Modulus Asphalt Mixes. In *Proceedings of the 3rd Eurasphalt and Eurobitume Congress*, Vienna, Austria, 2004.

Diefenderfer, B. K. and G. W. Maupin. *Field Trials of High-Modulus High-Binder-Content Base Layer Hot-Mix Asphalt Mixtures*. Report No. FHWA/VTRC 11-R2. Virginia Transportation Research Council, Charlottesville, Va., 2010.

Distin, T., L. Sampson, H. Marais, and B. Verhaeghe. *High Modulus Asphalt: Assessment of Viability Based on Outcomes of Overseas Fact Finding Mission*. White Paper, 2006.

European Asphalt Pavement Association. *Airfield uses of Asphalt*. Netherlands, 2003.

European Asphalt Pavement Association. *High Modulus Asphalt: A State of the Art Report*. Netherlands, 2005.

Guyot, X. Use of High Modulus Asphalt - "EME" Case Studies in the Indian Ocean Area. *15th AAPA International Flexible Pavements Conference*, Brisbane, Australia, 2013.

Haritonovs, V., J. Tihonovs, M. Zaumanis, and A. Krasnikovos. *High Modulus Asphalt Concrete with Dolomite Aggregate*. Transport Research Arena. Paris, France. 2014.

Hou, T., B. S. Underwood, and Y. R. Kim. Fatigue Performance Prediction of North Carolina Mixtures Using the Simplified Viscoelastic Continuum Damage Model. *Journal of the Association of Asphalt Paving Technologists*, Vol. 79, 2010, pp. 35-80.

Jacques, C., J. S. Daniel, T. Bennert, G. Reinke, A. Norouzi, C. Ericson, W. Mogawer, and Y. R. Kim. Effect of Silo Storage Time on the Characteristics of Virgin and Reclaimed Asphalt Pavement Mixtures. *Transportation Research Record: Journal of the Transportation Research Board*, No. 2573, Washington, D.C., 2016, pp. 76-85.

Jamois, D., J. C. Vaniscote, Y. Jolivet, and M. Malot. Development of a Concept of Very High Modulus Bituminous Macadam for Pavement Base Courses. *Proceedings of the 2nd Eurasphalt and Eurobitume Congress*, Vol. 2, Barcelona, Spain, 2000.

Lee, H. J., J. H. Lee, and H. M. Park. Performance Evaluation of High Modulus Asphalt Mixtures for Long Life Asphalt Pavements. *Construction and Building Materials*, Vol. 21, No. 5, 2007, pp. 1079-1087.

Lenfant, M. High Rutting Resistant Asphalt Pavement. *Seminar for Thailand Department of Highways*, TIPCO Asphalt Public Company Limited, Bangkok, Thailand, 269-289.

Michaut, J. P. *EME or High Modulus Asphalt Concrete*. COLAS Presentation. March 2014.

Miro, R., G. Valdés, A. Martinez, P. Segura, and C. Rodriguez. Evaluation of High Modulus Mixture Behavior with High Reclaimed Asphalt Pavement (RAP) Percentages for Sustainable Road Construction. *Construction and Building Materials*, Vol. 25, No. 10, 2011, pp. 3854-3862.

Montanelli, E. F. Fiber/Polymeric Compound for High Modulus Polymer Modified Asphalt (PMA). *Procedia-Social and Behavioral Sciences*, Vol. 104, 2013, pp. 39-48.

Newcomb, D. and K. Hansen. Mix Type Selection for Perpetual Pavements. Presented at the Perpetual Pavement Conference, Columbus, Ohio, 2004.

Newcomb, D. E., D. H. Timm, and R. Willis. *Perpetual Asphalt Pavements: A Synthesis*. Asphalt Pavement Alliance, Lanham, Md., 2010.

Nicholls, J. C., R. Elliott, N. Meite, R. Perera, A. Hunter, and J. Williams. Monitoring the Introduction of Enrobe a Module Eleve Class 2 onto UK Roads. In *Proceedings of the 4th Eurasphalt and Eurobitume Congress*, Copenhagen, Denmark, 2008.

Nkgapele, M., E. Denneman, and J. K. Anochie-Boateng. Construction of a High Modulus Asphalt (HiMA) Trial Section Ethekwini: South Africa's First Practical Experience with Design, Manufacturing and Paving of HiMA. Presented at 31st Southern African Transport Conference, Pretoria, South Africa, 2012.

Petho, L., and E. Denneman. High Modulus Asphalt Mix (EME) for Heavy Duty Applications and Preliminary Laboratory Test Results in Australia. Presented at 15th AAPA International Flexible Pavements Conference, Brisbane, Australia, 2013.

Rahbar-Rastegar, R., and J. S. Daniel. Laboratory versus Plant Production: Impact of Marerial Properties and Performance for RAP and RAS mixtures. International Journal of Pavement Engineering, 2016, pp. 1-12.

Sabouri, M., and Y. R. Kim. Development of a Failure Criterion for Asphalt Mixtures Under Different Modes of Fatigue Loading. In *Transportation Research Record: Journal of the Transportation Research Board*, No. 2447, Transportation Research Board of the National Academies, 2014, pp. 117-125.

Sanders, P. J., and M. Nunn. *The Application of Enrobe a Module Eleve in Flexible Pavements*. TRL Report TRL636, Transport Research Laboratory, Crowthorne, United Kingdom, 2005.

Underwood B., C. Baek, and Y. Kim. Simplified Viscoelastic Continuum Damage Model as Platform for Asphalt Concrete Fatigue Analysis. In Transportation Research Record: Journal of the Transportation Research Board, No. 2296, Transportation Research Board of the National Academies, 2012, pp. 36-45.

Vaitkus, A., and V. Vorobjovas. Use of Local Aggregate in High Modulus Asphalt Concrete Layers. *Gradevinar*, Vol. 65, No. 4, 2013, pp. 353-360.

Wei, O., F. Xinghua, and W. Lianguang. Research on Anti-Rutting Performance of High Modulus Asphalt Concrete Pavement. *Journal of Highway and Transportation Research and Development*, Vol. 4, No. 2, 2010, pp. 77-79.

Wielenski, J. C., and G. A. Huber. Evaluation of French High Modulus Asphalt (EME) in Pavement Structural Design (MEPDG). *Journal of the Association of Asphalt Paving Technologists*, Vol 80, 2011, pp 697-718.